A Stackelberg-Based Biomass Power Trading Game Framework in Hybrid-Wind/Solar/Biomass System: From Technological, Economic, Environmental and Social Perspectives

Yidan Huang[a,b], Qing Wang[b], Jiuping Xu[1 a,c]

[a]Business School, Sichuan University, Chengdu 610064, P. R. China
[b]Department of Engineering, Durham University, Stockton Road, DH1 3LE, Durham, the United Kingdom
[c]Institute of New Energy and Low-Carbon Technology, Sichuan University, Chengdu 610064, P. R. China

Abstract

Developing hybrid renewable energy systems (HRES) has been recognized as the best sustainable method for responding to global energy shortages. Introducing biomass power as backup into the HRES enables the improvement of the reliability of HRES powered by 100% renewable energy. But, the motivation behind this integration has been ignored and has inspired this study. In this study, a Stackelberg-based biomass power trading framework was designed to express resource integration and business collaboration between solar, wind, and biomass power operators for uninterrupted power feed-in. Subsequently, a bi-level multi-objective dynamics optimization model was developed to simulate the interplay between stakeholders in a hybrid 100% renewable energy system for the equilibrium between system reliability, profit requirements, environmental benefits, and social value. Finally, the biomass power trading framework and optimization method were successfully simulated in solar-wind-biomass HRES in the Qianjiang area, Chongqing City. The results demonstrated the effectiveness of the proposed methodology. The hybrid wind-solar-biomass renewable energy system could feed in power to the main grid around of 526 million kWh over the year, among which wind power contributes above 57%, and biomass power stations supply a quarter of the electricity. With 2.92% of unmet load rate, operators of HRES and biomass stations can improve their earnings by 0.02 and 0.06 CNY/per kWh compared to their actual operations, respectively. After the sensitivity analyses, valuable conclusions and suggestions about natural resource changes, power delivery strategies selection, and so on were drawn for reference by business operators and local authorities for the multi-dimensional sustainable development of HRES.

Keywords: Biomass power trading, Bio-waste treatment, Bi-level multi-objective optimization, Solar energy, Wind power;

1. Introduction

Global economic development and growing energy demand witnessed surging of CO_2 emissions over decades [1]. Grey electricity production has been recognized as a significant contributor to global warming effects, and its limited supply and rising cost also arouses social concerns [2]. Nowadays, taking a radical restructuring of the worldwide energy system is the only way to combat these negative impacts and energy shortage problem [3], which requires increasing renewable electricity share to replace the fossil power supply [4, 5]. However, most of these, especially wind and solar power, show variable availability with time, seasonality and daylong availability, and location, which have been recognized as not the optimal solution for these goals.

To solve the problem, a renewable energy revolution-hybrid renewable energy system (HRES) is quietly rising [6]. Fossil fuel generators, battery energy storage systems, and other power sources like biomass recovery are the potential candidates to be integrated with intermittent resources to ensure continuous access to electricity and energy security [7]. The diesel engine is prevalent in many rural or remote areas because of simple installation and control schemes [8]. But from a long-term perspective, the fuel cost, transportation cost, bulk storage need, and its environmental effects make it an unappealing option, especially with the sharp rise in diesel engine prices globally. Batteries are seen as a perfect backup for the hybrid renewable energy system. Still, they only allow for finite storage of power, and in the

[1]Corresponding author. *E-mail address*:xujiuping@scu.edu.cn.

long-term, this can be impractical as batteries can discharge and suffer degradation as they reach the end of their life span [9]. Consequently, academics shifted their attention to obtaining power from biodegraded resources, including kitchen waste, agriculture waste, and livestock manure with its vast potential, predictability, and controllability in power generation using anaerobic digestion and gasification [2]. Further, biomass recovery is environmentally friendly to ensure waste can be reasonably disposed of and reduce pollution released into the atmosphere and ecology [10].

Biomass power with controllability has been recognized as an appropriate sustainable backup for the hybrid solar-wind energy system, while HRES comprised of 100 % renewable energies is still complex and uncertain. To address these uncertain problems, many studies conducted multi-energy sources dispatch using optimization programming and commercial software from techno-economic-environmental perspectives [11]. For example, Colmenar-Santos et al. [10] found that concentrated solar power stations hybridized with biogas are technically feasible. This method is more economical than salt storage systems, as well as better operation time and electrical production control. Ghaem Sigarchian et al. [2] explored a hybrid power system consisting of photovoltaic panels, a wind turbine, and a biogas engine through a techno-economic analysis using HOMER. The simulation result shows that the hybrid system integrated with the biogas engine as a backup can be a better solution than using a diesel engine as a backup. The energy component structure is also considered in Liu et al. [1], while differently, the study takes an optimization modeling approach in which the system operating costs, waste disposal costs, and carbon trading costs are used as optimization objectives, presenting an economic dispatch based on robust stochastic optimization to reduce the operational difficulty of the integrated energy system. Beyond the technical, economic, and environmental advantages, Kushwaha et al. [12] highlighted that HRES, which integrates solar, wind, and biogas alongside conventional fossil fuels, can also yield significant social benefits, including job creation. However, the benefits that have been proven in these studies are based on the premise that biomass must feed its power into HRES. Namely, the endogenous motivation holding biomass power stations to join wind-solar power stations for collaboration has generally been ignored by previous authors.

Generally, biomass power stations receive a substantial income from the local authorities as they can sell reliable renewable electricity to the main grid [13, 14]. Therefore, a more attractive offer is an initial driver for biomass power stations to shift their current operation mode, feeding the generated electricity to HRES rather than the main grid for profits. In addition to a reasonable price, the power transmission amount is another critical factor influencing stakeholders' profits. Determining both the price and amount of biomass power is a complex process involving multi-stakeholders because they need to consider their demand and play with each other by adjusting their operational strategies to maximize their interests [15, 16]. It could be viewed as a typical Stackelberg game between suppliers and consumers in a market economy background and transformed into a mathematical form seeking equilibrium resolution [17]. Bi-level programming, widely used to express the interests of multiple stakeholders, has been proven to be one of the most potent tools for game resolution in many studies associated with the renewable power trade [18]. For example, Soares et al. [19] expressed an interaction between an electricity retailer and the consumer through a bi-level optimization model, where the leader determines the pricing scheme for benefits maximization, and the followers consider the demand and loads for discomfort and electricity bill minimization; Hua et al. [20] proposed a multi-energy pricing bi-level method for a biogas-solar renewable energy provider with heterogeneous consumers to interactively and dynamically determine the internal trading prices for optimal multi-energy trading between the provider and consumers. While bi-level programming presents a reliable capacity to solve pricing games revolving around the relationship of supply-demand in the electricity trade, there remains a gap in understanding how game theory can be applied to address specific problems faced by solar, wind, and biomass operators with individual expected goals. Furthermore, no study in this field tried to incorporate technological, economic, environmental, and social equilibria into game models and explore the interplay between these factors.

To fill the research gaps in the deployment and operation of hybrid wind/solar/biomass system, this study proposes a Stackelberg-based biomass power trading framework for a biomass power provider and operator of wind-solar power for reliable renewable electricity delivery, economic benefits, carbon reduction, and social value achievement. First, critical problems are recognized in deploying and operating the new HRES, after which a bi-level multi-objective dynamics model is developed to simulate these operation and business activities, maximizing technological-economic-environmental-social benefits for each stakeholder. And then, a kit of solving algorithms that integrates the ε-constraint method and Karush-Kuhn-Tucker (KKT) conditions is developed to seek the equilibrium result of these problems. Finally, the proposed method is applied to a practical case to demonstrate its applicability, where basic configuration and hourly dispatch over the whole year is presented, and scenario analyses related to the natural resource uncertainty, feed-in electricity pattern, and economical instrument are carried out by adjusting associated parameters. Over the discussion, propositions, and suggestions are made for all stakeholders to attain sustainable development.

In contrast to the existing literature, this study provides a tailored operations strategy involving multi-stakeholders with a more holistic perspective through problem identification, approach formulation, and practice application. The novelty goals are fourfold as represented as follows: (1) Building a collaboration strategy to integrate biomass with wind-solar power, which is a hybrid energy system fueled by 100% renewable energy, meaning an effective response to the fundamental restructuring of the traditional energy system. (2) developing a bi-level multi-objective dynamics model provides a comprehensive decision-making tool that simulates the power generation process in their operation period respectively and explores endogenous drivers, that is, biomass power trade game with flexible pricing. (3) designing a feasible solving algorithm to find reasonable prices and trade amounts of biomass power, which achieve a mutually beneficial outcome for each stakeholder from technological, economic, environmental, and social perspectives. (4) Conducting a case study to prove the advantages of the hybrid solar-wind-biomass energy system, demonstrate the feasibility and applicability of the proposed model and give practical power trade and dispatch strategy guidance from economic, technological, and societal perspectives for the stakeholders. To sum up, that is a systematic optimization paradigm, including power generation to mixed power dispatch planning, which is expected to be a reference for the potential user in other geographical locations.

2. Key problem statement

Before the model simulation of the HRES deployment and operation, critical problems should be recognized and summarized in three aspects, as follows; (1) dealing with uncertainty caused by intermittent wind-solar power, (2) considering game activities in bioelectricity trade, and (3) addressing adverse effects of seasonal harvest characteristics of biomass feedstock. These tailored solutions are depicted as Fig. 1.

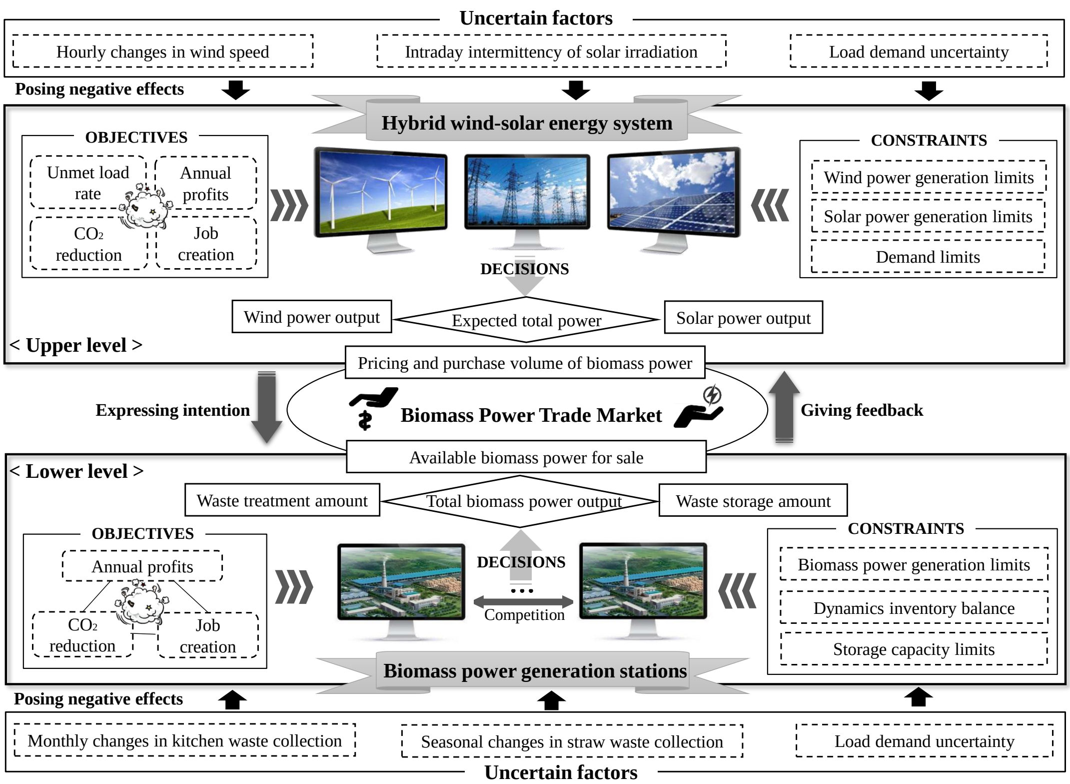

Figure 1: Development and application of the methodology

2.1. Methods to handle uncertainty of wind-solar resources

As shown in the upper part of Fig. 1, renewable power outputs of wind turbines and photovoltaic (PV) arrays change as long-term seasons and short-term weather increase main grid vulnerability [21, 22]. Even though natural complementarities among these renewable energy sources allow them to contribute more steady power output compared with a single source, the limits of HRES still exist in many scenarios; for example, summer nights or windless and cloudy days in winter do not have enough energy to drive the equipment for power generation. Integrating a storage system into the HRES has been characterized as adjusting capacity to output constant power by introducing fuel cells or constructing a hydropower station [23]. However, the repeated charging and discharging of batteries can lead to a discount in service life as well as rated capacity, and the laying batteries require a large amount of land surrounding the power equipment, and the chemical fuel used to make them may cause environmental pollution and safety threats. Besides, not all regions are suitable for hydropower station construction; forced construction can cause damage to local ecology, mainly geological and hydrological conditions. In addition, fossil power generators with controllability advantages are considered robust supporters of power supplements in case renewable resources are unavailable. But it is not to be ignored that fossil power generation contradicts the vision of sustainable development, which is an unsustainable development option. As a result, the research community has shifted its research to biomass. Because waste is considered to be steadily available throughout the year and can act as a continuous energy storage buffer [24]. The study thus proposes a wind-solar-biomass complementary approach to alleviate the scheduling pressures in renewable generations under a given demand target. The assessment covers the typical day data of each month in the whole year, which can cover most of the operation's regular and episodic weather occurrences and achieve a trade-off of economic and environmental benefits.

2.2. Stackelberg-based trade game to support biomass joining

A trading mechanism with a reasonable price helps to reach the collaboration of operators of a biopower and solar/wind energy system. The bio-electricity supplier will be attracted to trade their power with the HRES once its operator offers higher power prices; otherwise, they will spontaneously deal with the main grid as before. Therefore, there would arise a challenge in the interaction process between the demander and suppliers, where each participant strives to maximize their benefits. More details are shown in the middle part of Fig. 1; wind-solar hybrid system operators determine the agreed total power output to the main grid, after which they purchase an amount of biomass power through trading to counteract instability caused by varied natural weather conditions. Meanwhile, in response to expected demand, biomass power stations will design their waste-to-energy plan for power demanders on time.

A game theory-based mathematical model involving the price and trading volume game for biomass electricity is introduced and applied to simulate these complex activities in biomass-integrated HRES. The entire system can be viewed as a one-leader multi-follower Stackelberg game, where the demander (operator of HRES) and providers (Biomass power stations) act as leader and followers, respectively. First, the HRES operator will propose an initial offer including the price and volume of electricity purchased based on its output of wind and photovoltaic electricity for each period, taking into account the electricity demand in the market; subsequently, the biomass power station as followers will compare the offer with the subsidies granted by the main grid, given the objective of maximizing its operating profits, and pose responses about the distribution of waste disposal and electricity sold. Further, the decision of followers may disrupt the goals of the operator of HRES, such that the operators commensurately make feedback by adjusting their disposal and production plans again. This is an interactive non-cooperative game because all providers and demanders are generally self-interested and strive to maximize their objective benefits during power trading. After a finite number of n games, the final equilibrium solution acceptable to each participant in the energy market can be found.

2.3. Storage strategy for seasonable waste collection

Biomass power stations deploy various biotechnological or chemical techniques based on different waste characteristics to produce biofuels such as methane and hydrogen and generate electricity as the end-of-energy product using combined heat and power [9, 10]. Agriculture waste, mainly straw and livestock manure, and kitchen waste in urban areas have been identified as major waste sources with great potential for power output [25, 26]. As mentioned by the bottom part of Fig. 1, in addition to the monthly changes in kitchen waste generation, straw has a strong seasonality because it is closely related to crop stationing and harvesting. Namely, the straw waste substrate is just collected in the Autumn, which is quite different from the annual power demand. Besides, the yearly collection amount of straw is considerable, and its contribution to the biomass power sector cannot be ignored.

This study, therefore, introduces a storage strategy where the warehouses allow a reserve of straw waste generated to prepare for electricity conversion in the future. This strategy requires a certain economic expense, including storage and transportation. Still, its added value is also identified, such as more waste being recycled rather than directly incinerated. More flexible power output can be achieved because the decision-maker can call up the required substrate for power generation. Dynamic planning allows the decision maker to utilize each type of waste substrate based on the power generation demand for the best waste resource utilization and operating profit.

3. Modeling

In this section, the bi-level multi-objective (BLMO) optimization model is discussed at the mathematical level considering the economic, technological, environmental, and social aspects for each stakeholder.

3.1. Leader's objectives

The technical-economic-environmental-social objectives chosen for designing and operating HRES with dispatch strategies involved with biomass power trading are described further below, where unmet load rate (ULR), net profits (NP), carbon reduction (CR), and job creation (JC) are used as assessment indicators respectively.

Technological objective. A reliable power supply is essential for power-using security both for residential and industry, especially for hybrid energy systems supported by natural sources [27]. As stated in the key problem statement of this paper, wind, and solar power have unsatisfactory power output in many cases. Even though the scheduling center could regulate real-time peaking in the grid, frequent intermittent variations inevitably threaten the main grid, increasing vulnerability. Unmet load is normally used to assess the technical performance of a proposed system [12], shown in Eq. (1). Let UL_{kt} is daily unserved load value at time t in month k and $\sum_{k}^{K}\sum_{t}^{T} OD_{kt}^{E}$ refers to the daily agreed feed-in power. L_k refer to the days in month k. Therefore, the technological objective is assessed by minimizing annual ULR to guarantee that the real supplied power does not deviate much from the agreed output.

$$Min\ URL = \frac{\sum_{k}^{K} L_k \cdot \sum_{t}^{T} UL_{kt}}{\sum_{k}^{K} L_k \cdot \sum_{t}^{T} OD_{kt}^{E}} \tag{1}$$

Economic objective. The net profits are the most critical indicator for operators to evaluate whether the current deployment of HRES is economically feasible. It shows the annualized cash flow from HRES deployment and operations, including electricity trade net income from the main grid and biomass power stations, and the initial capital and operational and maintenance cost for each component [28]. First, because of the renewable energy generation incentive policy, these operators could be rewarded with a certain subsidy granted by the central government above the benchmark electricity price [29]. Let p^w, p^s, and p^b represent the unit subsidy for wind power, solar power, and biomass power; the amount of various renewable sources in station i, j and r could be calculated as Q_{kit}^{HRES}, Q_{kjt}^{HRES} and Q_{krt}^{HRES}. Here, biomass trading activities exist because biomass electricity that injects into the main grid is purchased from biomass power stations instead of being self-produced by HRES. This requires the upper operator to pose an acceptable offer (p^{b*} CNY/kWh) to purchase, and the net profits related to the trading game should be $Q_{krt}^{HRES} \cdot (p^b - p^{b*})$. In addition to revenue, the penalties item should be considered in net income accounting if the agreed power has not been met, equal to the product of the amount of the unserved load (UL_{kt}) and the unit fine f [30]. Further, the initial capital cost for each component is determined by the installed capacity [31]. The capital cost of construction and replacement for the unit equipped with a certain capacity is $A_i^w + B_i^w$ and $A_j^s + B_j^s$, and the number of wind turbines and photovoltaic (PV) arrays are $n_i^{\max}$ and $n_j^{\max}$ respectively. So, the annualized capital cost during the lifetime (T_i^w and T_j^s) is calculated by introducing the capital recovery factor [32], expressed as $\frac{A_i^w+B_i^w}{T_i^w \cdot CRF_{(i,T)}} \cdot n_i^{\max} + \frac{A_j^s+B_j^s}{T_j^s \cdot CRF_{(j,T)}} \cdot n_j^{\max}$. Finally, operation and maintenance cost is positively correlated with the number of equipment started in the current month k, which is obtained by $C_i^w \cdot q_{sta}^w \cdot n_{ki}^w + C_j^s \cdot q_{sta}^s \cdot n_{kj}^s$ [29]. To sum up, the objective function for the net profits (NP) is collated and expressed as follows.

$$\begin{aligned} Max\ NP = \ & \sum_k^K L_k \cdot \sum_t^T \left[\sum_i^I Q_{kit}^{HRES} \cdot p^w + \sum_j^J Q_{kjt}^{HRES} \cdot p^s + \sum_r^R Q_{krt}^{HRES} \cdot \left(p^b - p^{b*}\right) - UL_{kt} \cdot f \right] \\ & - \sum_i^I \left(\frac{A_i^w + B_i^w}{T_i^w \cdot CRF_{(i,T)}} \cdot n_i^{\max} + \sum_k^K C_i^w \cdot q_{sta}^w \cdot n_{ki}^w \right) - \sum_j^J \left(\frac{A_j^s + B_j^s}{T_j^s \cdot CRF_{(j,T)}} \cdot n_j^{\max} + \sum_k^K C_j^s \cdot q_{sta}^s \cdot n_{kj}^s \right) \end{aligned} \tag{2}$$

Environmental objective. Renewable energies have been characterized as clean and zero-carbon emission, which means that if used to replace traditional fuel could reduce CO_2 released into the global atmosphere [29]. Therefore, the total reduction of carbon emission over the study period could be calculated as $\varpi \cdot \sum_k^K L_k \cdot \sum_t^T \left(\sum_i^I Q_{kit}^{HRES} + \sum_j^J Q_{kjt}^{HRES} \right)$, where the ϖ is the average carbon emissions parameter for the coal burning generation process from the main grid. In addition, the carbon emission could be captured in the solar/wind power station, mainly resulting from the construction and production stages (84.92%) [33]. Carbon emission intensity is usually used to measure environmental performance in short/mid-term research, which expresses the carbon emissions associated with all life cycle stages of the solar/wind farm per unit of electricity production during the life cycle. Carbon emission for wind/solar power stations could be accounted as $\omega_i \cdot Q_{kit}^{HRES} + \omega_j \cdot Q_{kjt}^{HRES}$, where the ω_i and ω_j denote emission intensity level of station i and j respectively. To sum up, the total carbon emission reduction could be expressed as Eq. (3) over the study period.

$$Max\ CR = \varpi \cdot \sum_k^K L_k \cdot \sum_t^T \left(\sum_i^I Q_{kit}^{HRES} + \sum_j^J Q_{kjt}^{HRES} \right) - \sum_k^K L_k \cdot \sum_t^T \left(\sum_i^I \omega_i \cdot Q_{kit}^{HRES} + \sum_j^J \omega_j \cdot Q_{kjt}^{HRES} \right) \tag{3}$$

Social objective. Even though the social benefits are not discussed as much as tech-economic and environmental objectives in existing literature in the renewable energy field, it has been recognized as an important indicator for sustainable deployment framework [29, 34, 35], in which job creation is the most significant aspect for commercial power stations [36]. Therefore, in this paper, the number of accrued local jobs are employed to express the social benefits of wind-solar power stations in which those positions are created to support power station construction and daily operation and maintenance. Ref by Dufo-López et al. [37], if the JC_i and JC_j are the numbers of jobs created of the unit wind turbine with a rated capacity in station i and unit PV array in station j respectively, the total job creation could be accounted by Eq. (4).

$$Max\ JC = n_i^{\max} \cdot JC_i + n_j^{\max} \cdot JC_j \tag{4}$$

3.2. Leader's constraints

Constraints for each component are given in this subsection to express intrinsic limitations in the power output and trade.

Wind power output. The output characteristics of wind turbines mainly depend on wind speed. Referring to Wang et al. [29], power generation via wind turbines could present four statuses. If the real speed rate ($v_i(t)$) is lower than the cut-in speed v_i^{in} that is not enough for the turbine's operation, the output of the station i is 0 at time t. If the real speed rate is ranged at the available range $\left[v_i^{in}, v_i^{ra}\right]$, the unit output must be below its rated power, expressed as $q_{sta}^w \cdot \frac{v(t) - v_i^{in}}{v_i^{ra} - v_i^{in}}$ where q_{sta}^w is the rated energy of a turbine at the time t (kW) determined by the hub height and length, v_i^{ra} is rated wind speed. If the wind speed exceeds the rated speed of the wind turbines but is below the acceptable maximum speed at time t, the power output could reach the rated power output by adjusting the orientation of the wind turbine i. Finally, if the wind speed exceeds the cut-off wind speed of selected wind turbines (v_i^{out}), the system will turn off to protect the equipment. The above is the maximum value of electricity that can be converted per unit of wind turbine for a given wind condition, as the right side of Eq. (5), while the real power uploaded Q_{kit}^{HRES} is determined by the operator of wind power station i comprehensive based real wind condition and economic return, where n_{ki}^{w} is the actual number of wind turn-on turbines in month k.

$$Q_{kit}^{HRES} \leq \begin{cases} 0 & v_i(t) < v_i^{in} \text{ or } v_i(t) > v_i^{out} \\ n_{ki}^{w} \cdot q_{sta}^{w} \cdot \frac{v_i(t) - v_i^{in}}{v_i^{ra} - v_i^{in}} & v_i^{in} \leq v_i(t) \leq v_i^{ra} \\ n_{ki}^{w} \cdot q_{sta}^{w} & v_i^{ra} \leq v_i(t) \leq v_i^{out} \end{cases} \tag{5}$$

Here wind speed is usually measured at the height of the anemometer, but the power output of the wind turbine is calculated to be the wind speed at the height of the hub. So wind speed is further refined by $v_i(t) = v_i^0(t) \cdot \left(\frac{h}{h_0}\right)^g$ [38], where $v_i(t)$ and $v_i^0(t)$ are the speeds at the height of the hub and anemometer, and h and h_0 are the height of the hub and anemometer, g is a coefficient often set as 0.143.

Wind turbines limits. Eq. (6) guarantees that the number of turbines turned on at t time does not exceed the number of turbines installed at location i the beginning of the plan [39]. Due to technical constraints, the total output of the turbines at location i at time t should range in their available power range, which can be guaranteed by Eq. (7) [29].

$$n_{ki}^{w} \leq n_i^{\max} \tag{6}$$

$$N_i^{\min} \leq Q_{kit}^{HRES} \leq N_i^{\max} \tag{7}$$

Solar power output. The photovoltaic arrays absorb solar radiation and convert it to electrical energy. Solar power generated mainly depends on solar radiation and ambient temperature [40]. Referring to Li and Qiu [41], let n_{jt}^{s} be the photovoltaic arrays to be operated at solar site j at time t, and its rated power output refers to q_{sta}^{s}; S_{sta} denotes the solar irradiation in standard test conditions (generally as 1 kW/m^2) and using S_{kjt} expresses real observation value for solar irradiation in unit PV panel in the current time-step; Let T_{kjt} and T_{sta} be the actual air temperature at the photovoltaic power station where the solar modules are operating and standard temperature settled in the laboratory surrounding respectively, as well as τ is the temperature coefficient of the power output of solar cells, considered at $-0.35\%/°C$. Similar to wind power output, therefore, denote Q_{kjt}^{HRES} is the amount of electricity injected into the main grid by station j, its relationship with the output of solar power could be expressed as Eq. (8).

$$Q_{kjt}^{HRES} \leq n_{kj}^{s} \cdot q_{sta}^{s} \cdot \frac{S_{kjt}}{S_{sta}} \cdot \left[1 + \tau \cdot \left(T_{kjt} - T_{sta}\right)\right] \tag{8}$$

Photovoltaic arrays limits. Eq. (9) guarantees that the operated arrays at time t do not exceed available arrays installed in the solar site j; Further, because of the technology limitations, the total output amount for the site j at time t does not exceed the maximum rated power output and does not lower the minimum value of it, which could be assured by Eq. (10).

$$n_{kj}^{s} \leq n_j^{\max} \tag{9}$$

$$N_j^{\min} \leq Q_{kjt}^{HRES} \leq N_j^{\max} \tag{10}$$

Power balance for agreed power feed-in. The main grid will not choose to hoard power that is beyond the agreed received amount, nor will any private sector [42], which means that the operator would not deliver excess power above the agreed amount without revenue. Eq. (11) presents the hourly power balance between the agreed output, real wind/solar and biomass power output, and unserved load amount.

$$UL_{kt} + \sum_{i}^{I} Q_{kit}^{HRES} + \sum_{j}^{J} Q_{kjt}^{HRES} + \sum_{r}^{R} Q_{krt}^{HRES} = OD_{kt}^{E} \tag{11}$$

Agreed output power constraints. While grid-connected HRES is becoming increasingly popular worldwide, it cannot yet support the region's load demand on its own, a large proportion of which is supplied by other nonrenewable energy [43, 44]. Therefore, Eq. (12) guarantees the objective limits that the agreed amount (OD_{kt}^{E}) does not exceed the total load demand ($\widetilde{TD}_{kt}^{E}$).

$$OD_{kt}^{E} \leq \widetilde{TD}_{kt}^{E} \tag{12}$$

3.3. Followers' objective

Biomass power stations affiliated with Municipal Sanitation Group are responsible for waste clean recovery to produce renewable biomass power. Because of the stable collection rate of waste and the advantage of predictability, operators could coordinate their production plan to feed in reliable power. Therefore, they, as a follower in this bi-level game, will try to optimize their operation activities of biomass power generation for net profits, carbon emission reduction, and job creation maximization.

Economic objective. Net profits could be calculated by Eq. (13), which includes income from electricity trading and waste management, expenditure on waste collection and inventory, and an initial investment and daily operation cost in generator facilities. For electricity trade, the upper decision-maker would pose the unit price of p^{b*} to purchase the amount of biomass power Q_{krt}^{HRES} and the main grid would provide the subsidy p^{b} to accept the extra biomass power Q_{krt}^{BP}; the station could also obtain certain management fees for waste m, the local authorities determine that and then paid to generators, which could be represented as $\sum_{m}^{M} Q_{kr}^{m(in)} \cdot MR^{m}$ in operate period k [42]. Meanwhile, waste collection, inventory, and power conversion require capital support from operators [45]. The cost of transporting waste depends on several aspects, such as the transportation mode, distance traveled, the quantity of waste transported, and the actual routes taken by the vehicles. Generally, the waste collection area and the route traveled are fixed, while the daily quantity of waste transported varies during operation. Therefore, in this study, the transportation cost($\overline{TC}^{m}(\widehat{d}_{\cdot r})$) per unit flow of waste, including transportation and loading/unloading costs are used to multiply the daily collection amount($Q_{kr}^{m(in)}$) of waste m in month k for simplified the cost accounting without compromising objectivity [46, 47]. In addition, the waste that is sent to biomass power stations but is not treated in the current period will be stored for future power generation, which would generate several inventory fees. Inventory holding costs are calculated by multiplying the unit holding cost with the storage quantity at the beginning of each period in many models considered storage decisions and then summing the cost in the consecutive periods of the planning horizon. Different inventory holding cost parameters can be assumed for different biomass resources and storage systems with a certain capacity [48]. Therefore, let S_{kr}^{m} denote the inventory amount for waste m in month k, the station r has to pay the holding cost of $\sum_{m}^{M}(S_{kr}^{m} \cdot VC_{r}^{m})$ per day in month k, where VC_{r}^{m} is the unit holding costs for waste m of warehouse held by the operator of the station r [49]. The above daily income and expenditure items are multiplied by the number of days (L_k) each month and summed to calculate the annual profit amount. The last item caused by facilities operation, similar to the wind-solar power stations at the upper level, the operator of a biomass power station should be responsible for the facilities' deployment and waste management and recovery for the whole period, expressed as $\frac{A_r^b + B_r^b}{T_r^b} \cdot n_r^{\max} + \sum_{k}^{K} C_r^b \cdot n_{kr}^b$.

$$Max\ NP_r = \sum_{k}^{K} L_k \cdot \left[\sum_{t}^{T} (Q_{krt}^{HRES} \cdot p^{b*} + Q_{krt}^{BP} \cdot p^{b}) + \sum_{m}^{M} \left(MR^{m} \cdot Q_{kr}^{m(in)} - \overline{TC}^{m}(\widehat{d}_{\cdot r}) \cdot Q_{kr}^{m(in)} - S_{kr}^{m} \cdot VC_{r}^{m} \right) \right] - \left(\frac{A_r^b + B_r^b}{T_r^b} \cdot n_r^{\max} + \sum_{k}^{K} C_r^b \cdot n_{kr}^b \right) \tag{13}$$

Environmental objective. Similar to Eq. (3), saving carbon emission resulting from biomass power generated could also be obtained as $\varpi \cdot \sum_{k}^{K} L_k \cdot \sum_{t}^{T} (Q_{krt}^{HRES} + Q_{krt}^{BP})$. Direct/indirect carbon emission in waste collected transportation and inventory, as well as biomass power conversion activities, should be recognized, including this objective function, which is assumed to be proportional to the amount the waste collected [48]. First, Argo et al. [50] considered the emission function is linear concerning quantities shipped between nodes, for which carbon emission of a typical day for transportation activities per waste m could be calculated as $\overline{TE}^{m}(\widehat{d_{\cdot r}}) \cdot Q_{kr}^{m(in)}$. Second, the holding emission is generated by the use of utility (e.g., electricity, hot air), which depends on the inventory level and the storage time [48]. Here, let VE_r^m denote the carbon emission of holding per unit waste m, and the total emission for holding waste m could be expressed as $S_{kr}^{m} \cdot VE_r^m$ for each typical day in month k. Finally, the emission during biomass conversion is dependent on the type of biomass resources and conversion technologies, accounting as $DE_r^m \cdot \sum_{t}^{T} Q_{krt}^{m}$. To sum up, the carbon emission reduction for station r could be measured over the studied period by Eq. (14).

$$Max\ CR_r = \varpi \cdot \sum_{k}^{K} L_k \cdot \sum_{t}^{T} (Q_{krt}^{HRES} + Q_{krt}^{BP}) - \sum_{k}^{K} L_k \cdot \sum_{m}^{M} \left(\overline{TE}^{m}(\widehat{d_{\cdot r}}) \cdot Q_{kr}^{m(in)} + S_{kr}^{m} \cdot VE_r^m + DE_r^m \cdot \sum_{t}^{T} Q_{krt}^{m} \right) \quad (14)$$

Social objective objective. The social objective is set as similar to the upper level to maximize the accrued local jobs (full-time equivalent for a year) required activities associated with biomass power station r throughout the lifetime of the study. Jobs created during the construction and operation phases are explicitly considered in this model. First, the number of job positions to guarantee infrastructure, such as generation facilities (JC_r^{Fa}) and warehouses (JC_r^{Ho}), mainly depends on the capacity level and technological character of each facility deployed. And then the drivers needed are positively correlated with the shipped amount [47] because other factors are fixed, like the introduction for Eq. (13). Therefore, job creation could be measured by Eq. (15).

$$Max\ JC_r = JC_r^{Fa} \cdot n_r^{\max} + JC_r^{Ho} \cdot n_r^{Ho-\max} + \sum_{k}^{K} \sum_{m}^{M} \overline{TJ}^{m}(\widehat{d_{\cdot r}}) \cdot L_k \cdot Q_{kr}^{m(in)} \quad (15)$$

3.4. Constraints of follower

Biomass power output. Waste substrates are generally processed via two phases to obtain biomass power. First, from the waste substrate to biofuel, various waste, including kitchen waste, manure, and straw waste, are disposed of by anaerobic digestion or gasification to produce biogas or syngas accordingly [51, 52]. Let Q_{krt}^{m} be the total amount of type m waste that is used to produce power at station r at time t, and $VS^m\%$ is its total organic matter content (volatile solids) in the raw material. If δ_r^m is the specific gas output efficiency achieved by station r from the organic matter m (m^3/ton), the amount of biofuel would be expressed to $Q_{krt}^{m} \cdot VS^m\% \cdot \delta_r^m$. Further, these biofuels could produce electrical power via biomass electrical generation units, where the specific heat energy obtainable from the raw material is ψ_r (kWh/m^3). Consider during the hour Δt between period t to $t+1$, the relationship among output for HRES Q_{krt}^{HRES} and the main grid Q_{krt}^{BP} and waste utilization potential could be introduced by Eq. (16).

$$Q_{krt}^{HRES} + Q_{krt}^{BP} = \frac{\sum_{r}^{R} \sum_{m}^{M} Q_{krt}^{m} \cdot VS^m\% \cdot \delta_r^m \cdot \psi_r}{\Delta t} \quad (16)$$

Disposal capacity limits. Eq. (17) ensures waste treatment amount would not exceed the rated capacity of the biogas/syngas generator [53], where n_{kr}^{b} expresses the facilities is operated in month k. And Eq. (18) guarantees that the operated facilities have been deployed at the beginning.

$$\underline{q}_r^m \cdot n_{kr}^b \leq Q_{krt}^m \leq \overline{q}_r^m \cdot n_{kr}^b \tag{17}$$

$$n_{kr}^b \leq n_r^{\max} \tag{18}$$

Dynamic waste inventory. Eq. (19) expresses waste inventory status to show the relationship between the collected volume of waste m, inventory amount at the warehouse, and the amount of waste sent to the treatment line in each period [54]. S_{kr}^m is the initial storage amount for waste m in the warehouse determined by power station r in month k, $Q_{kr}^{m(in)}$ is daily incoming amount of waste m that station r is willing to receive for disposing of in month k and Q_{krt}^m is the disposed of the waste amount of station r at the same period.

$$S_{kr}^m = \begin{cases} (Q_{kr}^{m(in)} - \sum_t^T Q_{krt}^m) \cdot L_k & k = 1 \\ S_{k-1,r}^m + (Q_{kr}^{m(in)} - \sum_t^T Q_{krt}^m) \cdot L_k & k \geq 2 \end{cases} \tag{19}$$

Waste flowing limits. Eq. (20) limits that the sum of the waste quantities of received of at each station r does not exceed the total demand of waste disposed $\widetilde{TD}_k^m$ [55].

$$\sum_r^R Q_{kr}^{m(in)} \leq \widetilde{TD}_k^m \tag{20}$$

Inventory capacity limit. Eq. (21) guarantees that the amount of the stored waste m does not exceed the available storage capacity in station r at any time [54].

$$\underline{S}_r^m \leq S_{kr}^m \leq \overline{S}_r^m \tag{21}$$

Integrate constraint. Eq. (22) guarantees the nonnegative nature of the decision variables.

$$n_{ki}^w, n_{kj}^s, n_{kr}^b \in N \tag{22}$$

Non-negative constraint. Eq. (23) guarantees the nonnegative nature of the decision variables.

$$Q_{kit}^{HRES}, Q_{kjt}^{HRES}, Q_{krt}^{HRES}, Q_{krt}^{BP}, Q_{kr}^{m(in)}, Q_{krt}^m \geq 0 \tag{23}$$

3.5. Global model

The paper develops a new collaboration mode involving the traditional hybrid energy system and biomass power stations for more clean and steady power output. The operator at the upper level first determines sale quantities of wind power and solar power ($Q_{kit}^{HRES} + Q_{kjt}^{HRES}$), after which is proposed the initial purchase quantity (Q_{krt}^{HRES}) and unit price of biopower (p^{b*}) from the biomass power station r. Meanwhile, the biomass power stations would make their waste recovery and storage workload within their capacity constraints, energy balance, and total demand limits. All generated biomass power would be distributed either send to the main grid (Q_{krt}^{BP}) or the HRES (Q_{krt}^{HRES}), which could be influenced by the purchase offer with the unit price of p^{b*}. Further, the leader will adjust his initial decisions according to the response from the biomass power station, giving a new operating strategy in solar and wind power ($Q_{kit}^{HRES}, Q_{kjt}^{HRES}$) as well as purchase amount of biomass power with a certain price ($Q_{krt}^{HRES} \cdot p^{b*}$). Finally, the interaction process stops until all stakeholders reach a consensus or when the equilibrium solution is found [56].

$$
\begin{array}{l}
Min\ URL = \frac{\sum\limits_{k}^{K} L_k \cdot \sum\limits_{t}^{T} UL_{kt}}{\sum\limits_{k}^{K} L_k \cdot \sum\limits_{t}^{T} OD_{kt}^{E}} \\
Max\ NP = \sum\limits_{k}^{K} L_k \cdot \sum\limits_{t}^{T} \left[\sum\limits_{i}^{I} Q_{kit}^{HRES} \cdot p^{w} + \sum\limits_{j}^{J} Q_{kjt}^{HRES} \cdot p^{s} + \sum\limits_{r}^{R} Q_{krt}^{HRES} \cdot \left(p^{b} - p^{b*} \right) - UL_{kt} \cdot f \right] \\
- \sum\limits_{i}^{I} \left(\frac{A_i^w + B_i^w}{T_i^w \cdot CRF_{(i,T)}} \cdot n_i^{\max} + \sum\limits_{k}^{K} C_i^w \cdot q_{sta}^{w} \cdot n_{ki}^{w} \right) - \sum\limits_{j}^{J} \left(\frac{A_j^s + B_j^s}{T_j^s \cdot CRF_{(j,T)}} \cdot n_j^{\max} + \sum\limits_{k}^{K} C_j^s \cdot q_{sta}^{s} \cdot n_{kj}^{s} \right) \\
Max\ CR = \varpi \cdot \sum\limits_{k}^{K} L_k \cdot \sum\limits_{t}^{T} \left(\sum\limits_{i}^{I} Q_{kit}^{HRES} + \sum\limits_{j}^{J} Q_{kjt}^{HRES} \right) - \sum\limits_{k}^{K} L_k \cdot \sum\limits_{t}^{T} \left(\sum\limits_{i}^{I} \omega_i \cdot Q_{kit}^{HRES} + \sum\limits_{j}^{J} \omega_j \cdot Q_{kjt}^{HRES} \right) \\
Max\ JC = n_i^{\max} \cdot JC_i + n_j^{\max} \cdot JC_j \\
s.t. \left\{ \begin{array}{l}
Q_{kit}^{HRES} \le \left\{ \begin{array}{ll} 0 & v_i(t) < v_i^{in} \mathrm{or} v_i(t) > v_i^{out} \\ n_{ki}^{w} \cdot q_{sta}^{w} \cdot \frac{v_i(t) - v_i^{in}}{v_i^{ra} - v_i^{in}} & v_i^{in} \le v_i(t) \le v_i^{ra} \\ n_{ki}^{w} \cdot q_{sta}^{w} & v_i^{ra} \le v_i(t) \le v_i^{out} \end{array} \right. \\
n_{ki}^{w} \le n_i^{\max} \\
N_i^{\min} \le Q_{kit}^{HRES} \le N_i^{\max} \\
Q_{kjt}^{HRES} \le n_{kj}^{s} \cdot q_{sta}^{s} \cdot \frac{S_{kjt}}{S_{sta}} \cdot \left[1 + \tau \cdot \left(T_{kjt} - T_{sta} \right) \right] \\
n_{kj}^{s} \le n_j^{\max} \\
N_j^{\min} \le Q_{kjt}^{HRES} \le N_j^{\max} \\
UL_{kt} + \sum\limits_{i}^{I} Q_{kit}^{HRES} + \sum\limits_{j}^{J} Q_{kjt}^{HRES} + \sum\limits_{r}^{R} Q_{krt}^{HRES} = OD_{kt}^{E} \\
OD_{kt}^{E} \le \widetilde{TD}_{kt}^{E} \\
Max\ NP_r = \sum\limits_{k}^{K} L_k \cdot \left[\sum\limits_{t}^{T} (Q_{krt}^{HRES} \cdot p^{b*} + Q_{krt}^{BP} \cdot p^{b}) + \sum\limits_{m}^{M} \left(MR^{m} \cdot Q_{kr}^{m(in)} - \overline{TC}^{m} (\widehat{d}_{\cdot r}) \cdot Q_{kr}^{m(in)} - S_{kr}^{m} \cdot VC_r^{m} \right) \right] \\
- \left(\frac{A_r^b + B_r^b}{T_r^b} \cdot n_r^{\max} + \sum\limits_{k}^{K} C_r^b \cdot n_{kr}^{b} \right) \\
Max\ CR_r = \varpi \cdot \sum\limits_{k}^{K} L_k \cdot \sum\limits_{t}^{T} (Q_{krt}^{HRES} + Q_{krt}^{BP}) - \sum\limits_{k}^{K} L_k \cdot \sum\limits_{m}^{M} \left(\overline{TE}^{m} (\widehat{d}_{\cdot r}) \cdot Q_{kr}^{m(in)} + S_{kr}^{m} \cdot VE_r^{m} + DE_r^{m} \cdot \sum\limits_{t}^{T} Q_{krt}^{m} \right) \\
Max\ JC_r = JC_r^{Fa} \cdot n_r^{\max} + JC_r^{Ho} \cdot n_r^{Ho-\max} + \sum\limits_{k}^{K} \sum\limits_{m}^{M} \overline{TJ}^{m} (\widehat{d}_{\cdot r}) \cdot L_k \cdot Q_{kr}^{m(in)} \\
s.t. \left\{ \begin{array}{l}
Q_{krt}^{HRES} + Q_{krt}^{BP} = \frac{\sum\limits_{r}^{R} \sum\limits_{m}^{M} Q_{krt}^{m} \cdot VS^{m}\% \cdot \delta_r^{m} \cdot \psi_r}{\Delta t} \\
\underline{q}^{m} \cdot n_{kr}^{b} \le Q_{krt}^{m} \le \overline{q}^{m} \cdot n_{kr}^{b} \\
n_{kr}^{b} \le n_r^{\max} \\
S_{kr}^{m} = \left\{ \begin{array}{ll} (Q_{kr}^{m(in)} - \sum\limits_{t}^{T} Q_{krt}^{m}) \cdot L_k & k = 1 \\ S_{k-1,r}^{m} + (Q_{kr}^{m(in)} - \sum\limits_{t}^{T} Q_{krt}^{m}) \cdot L_k & k \ge 2 \end{array} \right. \\
\underline{S}_{rt}^{m} \le S_{kr}^{m} \le \overline{S}_{rt}^{m} \\
\sum\limits_{r}^{R} Q_{kr}^{m(in)} \le \widetilde{TD}_{k}^{m} \\
Q_{it}^{HRES}, Q_{jt}^{HRES}, Q_{rt}^{HRES}, Q_{krt}^{w}, Q_{rt}^{BP}, Q_{kr}^{m(in)} \ge 0 \\
n_{ki}^{w}, n_{kj}^{s}, n_{kr}^{b} \in N
\end{array} \right.
\end{array} \right.
\end{array}
\tag{24}
$$

The method seeks an equilibrium of BLMO in which multiple logical decision-makers try to maximize their self-interest based on their respective positions. This is a complex decision game involving multiple benefits and conflicts. First, the biomass power integrated wind-solar power stations need to simultaneously minimize *ULR* and maximize *NP*, *CR*, and *JC* during the operation period of HRES. The second conflict is between the operator of the wind-solar power stations and the biomass power stations, which is inspired by the first conflict and because of different self-interests. The operator of HRES, who pursues reliability of energy support and other objectives, needs to build collaboration with the biomass power station, while the profits objective requires decision makers to control the trade cost in this business negotiation. This is contrary to the intentions of lower-level decision makers because the stations must want to increase the unit revenue of power products as much as possible for their economic-environmental-social objectives maximization ($Max\ NP_r$, $Max\ CR_r$, $Max\ JC_r$). To resolve the conflict in this typical Stackelberg game, the decision-makers need to understand the intentions of others and constantly adjust their own operating strategies until the proposed mathematical model reaches maximum equilibrium for each decision-maker under the given constraints. Therefore, the proposed model (shown in Eq. (24)) integrates the power output and trade from various sources, conflict analyses, and technological feasibility to reach an equilibrium of techno-economic, environmental, and social benefits.

3.6. Model solution method

The proposed model shown in Eq. (24) represents the goals of the wind-solar and biomass power stations and reflects their complex mutual relationships. However, BLMO problems are non-deterministic polynomial time (NP)-hard problems and difficult to deal with, for which the improved ε-constraint method integrated with the KKT conditions is used to convert the BLMO into a single-objective, single-level model. The details of this transformation process are explained in the following.

3.6.1. ε-constraint method for multi-objective problem resolution

As the presentation of Eq. (24), there is a conflict in the nature between technical-economic-social-environmental objectives, which means that the decision-makers cannot find the "best" solution in the decision-making environment. ε-constraint method, which has been proven to be very efficient in multi-objective conflicts, guarantees one objective to be the ideal value and gives certain considerations to other objectives [57]. In this work, the economic objective is assumed as the primary objective for stakeholders at each level, while the technological, environmental objective and social objectives are transformed into the constraint conditions. In actual operation, the main grid has the certain regulation capability to resist risk caused by demand and supply uncertainty. However, frequent and excessive fluctuations still would lead to the collapse of the power system affecting grid security [30]. Therefore, according to the power trade and delivery characteristics, keeping the established and actual power delivery volumes for each time t within acceptable limits can regard the system as reliable. For environmental and social objectives, different decision-makers have different expectation levels for carbon emission reduction and job creation. So five parameters are introduced to represent system decision makers' altitude towards these objectives: ε^{URL} as the highest unmet load bound, ε^{CRu} and ε^{CRl} as the lowest carbon emission reduction bound of decision-makers at the upper level and lower level respective, and as well as the lowest bound of job creation (ε^{JCu} and ε^{JCl}). Then the multi-objective model can be transformed as Eq. (25).

$$
\begin{aligned}
& Max\ NP = \sum_{k}^{K} L_k \cdot \sum_{t}^{T} \left[\sum_{i}^{I} Q_{kit}^{HRES} \cdot p^{w} + \sum_{j}^{J} Q_{kjt}^{HRES} \cdot p^{s} + \sum_{r}^{R} Q_{krt}^{HRES} \cdot \left(p^{b} - p^{b*}\right) - UL_{kt} \cdot f \right] \\
& - \sum_{i}^{I} \left(\frac{A_i^w + B_i^w}{T_i^w \cdot CRF_{(i,T)}} \cdot n_i^{\max} + \sum_{k}^{K} C_i^w \cdot q_{sta}^{w} \cdot n_{ki}^{w} \right) - \sum_{j}^{J} \left(\frac{A_j^s + B_j^s}{T_j^s \cdot CRF_{(j,T)}} \cdot n_j^{\max} + \sum_{k}^{K} C_j^s \cdot q_{sta}^{s} \cdot n_{kj}^{s} \right) \\
& \left\{ \begin{array}{l}
URL \leq \varepsilon^{URL}, \quad CR \geq \varepsilon^{CRu}, \quad JC \geq \varepsilon^{JCu} \\
\text{Eqs. (5) – (12)} \\
Max\ NP_r = \sum_{k}^{K} L_k \cdot \left[\sum_{t}^{T} (Q_{krt}^{HRES} \cdot p^{b*} + Q_{krt}^{BP} \cdot p^{b}) + \sum_{m}^{M} \left(MR^m \cdot Q_{kr}^{m(in)} - \overline{TC}^{m}(\widehat{d}_{\cdot r}) \cdot Q_{kr}^{m(in)} - S_{kr}^{m} \cdot VC_r^m \right) \right] \\
- \left(\frac{A_r^b + B_r^b}{T_r^b} \cdot n_r^{\max} + \sum_{k}^{K} C_r^b \cdot n_{kr}^{b} \right) \\
CR_r \geq \varepsilon_r^{CRl}, \quad JC_r \geq \varepsilon_r^{JCl} \\
\text{Eqs. (16) – (23)}
\end{array} \right.
\end{aligned} \tag{25}
$$

3.6.2. KKT conditions for bi-level programming resolution

Ben-Ayed and Blair [58] proposed that the simplest game would become difficult to solve upon being involved with bi-level programming. To solve it, many meta-heuristics have been proposed in previous research, one of which

KKT optimal conditions is typical transformation mathematical theory widely used to successfully convert bi-level problems into single-level problems [59, 60]. The method requires the displacement of the lower-level problem with corresponding KKT conditions, which it then appends to the leader-level problem [61, 62]. The proposed bi-level model presents a business game with pricing for biomass power, where the core decision is the biomass power purchase amount, and other decisions, including wind-solar power output, the waste amount for treatment and s-torage, and facilities operation, would influence the core decision in this game. Therefore, a Lagrange multiplier $u_r^1, u_{krt}^1, u_{km}^1, ...$ was imported, with $g_r^1, g_{krt}^1, g_{km}^1, ...$ being the Lagrange function. Once the KKT conditions are satisfied, the conflict between the authority and the KW disposal stations is resolved, and the global satisfaction solution is found. Therefore, using the constraints method and the KKT optimal conditions, the bi-level multi-objective model was transformed into a single-level single-objective model in Eq. (26).

$$
\begin{aligned}
&Max\ NP = \sum_k^K L_k \cdot \sum_t^T \left[\sum_i^I Q_{kit}^{HRES} \cdot p^w + \sum_j^J Q_{kjt}^{HRES} \cdot p^s + \sum_r^R Q_{krt}^{HRES} \cdot \left(p^b - p^{b*}\right) - UL_{kt} \cdot f \right] \\
&- \sum_i^I \left(\frac{A_i^w + B_i^w}{T_i^w \cdot CRF_{(i,T)}} \cdot n_i^{\max} + \sum_k^K C_i^w \cdot q_{sta}^w \cdot n_{ki}^w \right) - \sum_j^J \left(\frac{A_j^s + B_j^s}{T_j^s \cdot CRF_{(j,T)}} \cdot n_j^{\max} + \sum_k^K C_j^s \cdot q_{sta}^s \cdot n_{kj}^s \right) \\
&\left\{
\begin{array}{l}
URL \le \varepsilon^{URL}, \quad CR \ge \varepsilon^{CRu}, \quad JC \ge \varepsilon^{JCu} \\
\frac{\partial g_r^0\left(Q_{krt}^{HRES}, Q_{krt}^m, Q_{kr}^{m(in)}, n_{kr}^b\right)}{\partial Q_{krt}^{HRES}} + u_r^1 \cdot \frac{\partial g_r^1\left(Q_{krt}^{HRES}, Q_{krt}^m, Q_{kr}^{m(in)}\right)}{\partial Q_{krt}^{HRES}} + u_{krt}^1 \cdot \frac{\partial g_{krt}^1\left(Q_{krt}^{HRES}, Q_{krt}^m\right)}{\partial Q_{krt}^{HRES}} = 0 \\
\frac{\partial g_r^0\left(Q_{krt}^{HRES}, Q_{krt}^m, Q_{kr}^{m(in)}, n_{kr}^b\right)}{\partial Q_{krt}^m} + u_r^1 \cdot \frac{\partial g_r^1\left(Q_{krt}^{HRES}, Q_{krt}^m, Q_{kr}^{m(in)}\right)}{\partial Q_{krt}^m} + u_{krt}^1 \cdot \frac{\partial g_{krt}^1\left(Q_{krt}^{HRES}, Q_{krt}^m\right)}{\partial Q_{krt}^m} + u_{krm}^2 \cdot \frac{\partial g_{krm}^2\left(Q_{kr}^{m(in)}, Q_{krt}^m\right)}{\partial Q_{krt}^m} + u_{krmt}^3 \cdot \frac{\partial g_{krmt}^3\left(Q_{krt}^m, n_{kr}^b\right)}{\partial Q_{krt}^m} = 0 \\
\frac{\partial g_r^0\left(Q_{krt}^{HRES}, Q_{krt}^m, Q_{kr}^{m(in)}, n_{kr}^b\right)}{\partial Q_{kr}^{m(in)}} + u_r^1 \cdot \frac{\partial g_r^1\left(Q_{krt}^{HRES}, Q_{krt}^m, Q_{kr}^{m(in)}\right)}{\partial Q_{kr}^{m(in)}} + u_r^2 \cdot \frac{\partial g_r^2\left(Q_{kr}^{m(in)}\right)}{\partial Q_{kr}^{m(in)}} + u_{km}^1 \cdot \frac{\partial g_{km}^1\left(Q_{kr}^{m(in)}\right)}{\partial Q_{kr}^{m(in)}} + u_{krm}^2 \cdot \frac{\partial g_{krm}^2\left(Q_{kr}^{m(in)}, Q_{krt}^m\right)}{\partial Q_{kr}^{m(in)}} = 0 \\
\frac{\partial g_r^0\left(Q_{krt}^{HRES}, Q_{krt}^m, Q_{kr}^{m(in)}, n_{kr}^b\right)}{\partial n_{kr}^b} + u_{krmt}^3 \cdot \frac{\partial g_{krmt}^3\left(Q_{krt}^m, n_{kr}^b\right)}{\partial n_{kr}^b} = 0 \\
g_r^0 = \sum_k^K L_k \cdot \left[\sum_t^T (Q_{krt}^{HRES} \cdot p^{b*} + Q_{krt}^{BP} \cdot p^b) + \sum_m^M \left(MR^m \cdot Q_{kr}^{m(in)} - \overline{TC}^m(\widehat{d}_{\cdot r}) \cdot Q_{kr}^{m(in)} - S_{kr}^m \cdot VC_r^m \right) \right] - \left(\frac{A_r^b + B_r^b}{T_r^b} \cdot n_r^{\max} + \sum_k^K C_r^b \cdot n_{kr}^b \right) \\
g_r^1 = \varpi \cdot \sum_k^K L_k \cdot \sum_t^T (Q_{krt}^{HRES} + Q_{krt}^{BP}) - \sum_k^K L_k \cdot \sum_m^M \left(\overline{TE}^m(\widehat{d}_{\cdot r}) \cdot Q_{kr}^{m(in)} + S_{kr}^m \cdot VE_r^m + DE_r^m \cdot \sum_t^T Q_{krt}^m \right) - \varepsilon_r^{CRl} \\
g_r^2 = JC_r^{Fa} \cdot n_r^{\max} + JC_r^{Ho} \cdot n_r^{Ho-\max} + \sum_k^K \sum_m^M \overline{TJ}^m(\widehat{d}_{\cdot r}) \cdot L_k \cdot Q_{kr}^{m(in)} - \varepsilon_r^{JCl} \\
g_{krt}^1 = \frac{\sum_m^M Q_{krt}^m \cdot VS^w\% \cdot \delta_r^m \cdot \psi_r}{\Delta t} - Q_{krt}^{BP} - Q_{krt}^{HRES} \\
g_{km}^1 = TD_k^m - \sum_r^R Q_{kr}^{m(in)} \\
g_{krm}^2 = \left\{ \begin{array}{ll} \overline{S}_r^m - (Q_{kr}^{m(in)} - \sum_t^T Q_{krt}^m) \cdot L_k & k = 1 \\ \overline{S}_r^m - S_{kr}^m - S_{k-1,r}^m - (Q_{kr}^{m(in)} - \sum_t^T Q_{krt}^m) \cdot L_k & k \ge 2 \end{array} \right. \\
g_{krmt}^3 = \overline{q}_t^m \cdot n_{kr}^b - Q_{krt}^m \\
\sum_r^R u_r^1 \cdot g_r^1 + \sum_r^R u_r^2 \cdot g_r^2 + \sum_k^K \sum_r^R \sum_t^T u_{krt}^1 \cdot g_{krt}^1 + \sum_k^K \sum_m^M u_{km}^1 \cdot g_{km}^1 + \sum_k^K \sum_r^R \sum_m^M u_{krm}^2 \cdot g_{krm}^2 + \sum_k^K \sum_r^R \sum_m^M \sum_t^T u_{krmt}^3 \cdot g_{krmt}^3 = 0 \\
u_r^1, u_r^2, u_{krt}^1, u_{km}^1, u_{krm}^2, u_{krmt}^3 \ge 0 \\
\text{Eqs.(5)} - (12)\ \&\ (16) - (23).
\end{array}
\right.
\end{aligned}
\tag{26}
$$

4. Case Study

In this section, a practical case study from the Qianjiang area, Chongqing city, China, is given to demonstrate the applicability of the proposed approach. After data collection, processing, and analysis, suggestions are supplied for each stakeholder and potential applier in similar real-life cases.

4.1. Case representation

With the urbanization in recent years, kitchen waste presents a high daily output value in Chongqing. And, Chongqing is also one of the seven major grain-producing areas in China. Therefore, there is also a huge potential for development in agricultural waste utilization [49]. Qianjiang, a district under the jurisdiction of Chongqing Municipality, is located southeast of Chongqing. The local authority in this area is actively implementing the concept of a waste-free city, promoting solid waste "reduction, resourcefulness and harmlessness" from the source, and playing a demonstration role in promoting the green development of the Yangtze River Economic Belt [63]. In addition to a lot of advanced biomass power stations with advanced waste resource recovery equipment, local governments have also actively deployed photovoltaic projects and wind power projects for renewable energy development. Therefore, this district is chosen to take a case study in this paper.

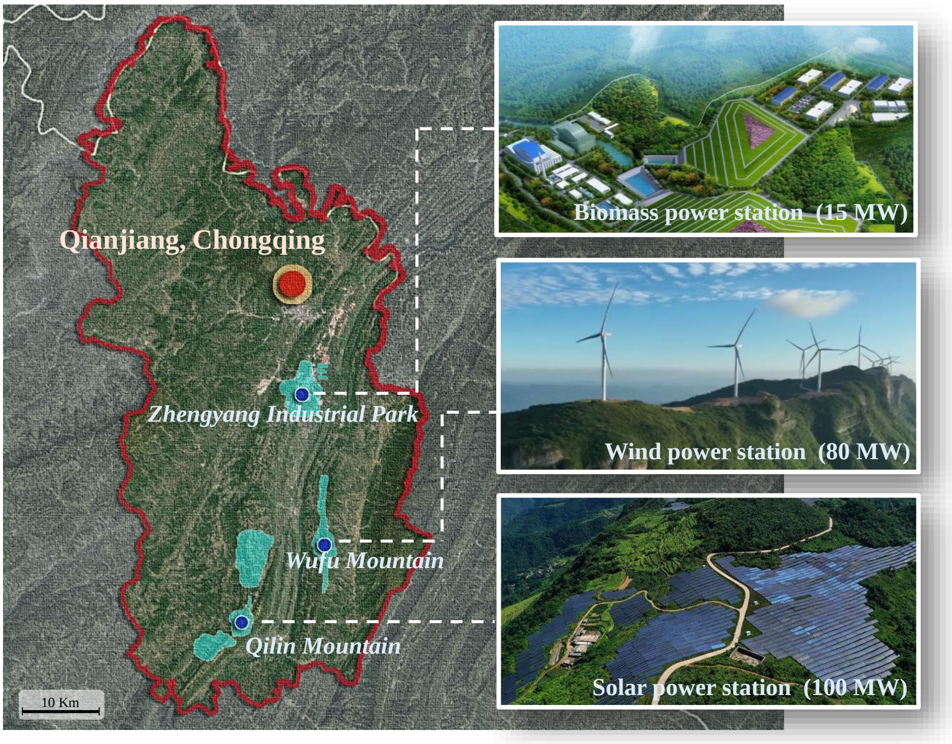

Figure 2: Case study location

Fig. 2 presents an overview of HRES components and the Qianjiang district. A biomass power station is located at Zhengyang industrial park in the center of the district covering an area of 13.9 km^2, where the total rated power of generators reaches 15 MW and an annual operation time of more than 8000 hours. A 100 MW solar power station is located on Qilin mountain, Qianjiang District, and is the first large-scale alpine power station in Chongqing. The project deploys 300,000 PV solar panels and covers an area of 1.22 km^2 at an altitude of nearly 1,500 m. On another mountain named Wufu, between 1,350 and 1,610 meters above sea level, wind turbines of the mountain type are installed, with a total rated power of 80 MW, comprised of 23 wind turbines with a power range of 3.3 MW to 3.6 MW.

4.2. Data collection

Before conducting the case study, relevant data for natural conditions and each component were collected. The typical hourly solar irradiation on Qilin mountain each month is shown in Fig. 3(a), which is collected from the GLOBAL SOLAR ATLAS website [64]. The typical hourly wind speed data were collected from the wind survey station on Wufu mountain and are shown in Fig. 3(b). The daily average waste generation potential and typical hourly power demand are presented in Fig. 3(c) and (d) from annual reports of the local ecological environment and power supply bureaus in 2021.

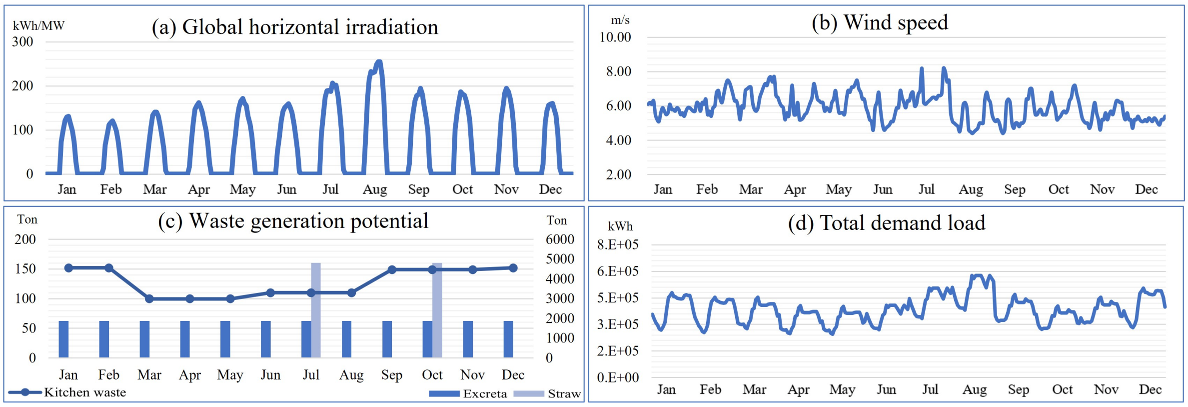

Figure 3: Typical daily irradiation, wind, waste potential and demand load profiles (24h)

The technological-environmental parameters of PV arrays, wind turbines, and biomass generator systems are introduced in Table B.1. And the economic-social parameters of these components are shown in Table B.2. Because of the fixed collection scope and route, needed data related to waste collection and inventory could be drawn (Table B.3) based on the maximum one-way collection distances (5.4, 8.7, and 23.4 km) for kitchen, manure and straw waste, respectively. According to the notice of wind power feed-in issued by [65], the wind power feed-in price in Chongqing is 0.47 CNY/kWh (Zone IV). Similarly, China National Development and Reform Commission [66] determines to award those stations that use "Surplus power feed-in trade mode" an additional 0.10 CNY/kWh solar power subsidy on top of the base price of fossil electricity feed-in tariff, a total 0.4964 CNY/kWh [67]. The price for biomass power is set at 0.6464 CNY/kWh [68].

4.3. Results of basic case

The transformed model in Eq. (26) is encoded into Lingo 17.0 software that presents capacity in dealing with complex calculation processes [69]. In addition to the collected data, some technological and economic parameters are needed for solving the model in the basic case, where let the agreed hourly power output is 16% of the hourly demand load, the price of biomass power trade is 0.7464 CNY/kWh, and unit fine for unserved load between real and agreed output is 0.8 CNY/kWh. After 42 seconds of processing 2910 constraints with 4871 variables, the optimal configuration is listed in Table 1. Further, hourly power contributed from solar-wind-biomass power is presented in Fig. 4.

Table 1: Optimal resolution of the basic case

Objectives value	Unmet load rate	Annual net profits (CNY)	CO_2 emission reduction (Kg)	Job creation	Annual power fed in (kWh)
Upper level	2.92%	135,284,087.05	80,313,980.92	326.3	526,071,983
Lower level	-	140,710,557.20	16,301,859.40	407.0	228,715,916
Waste recovery (tons)	Kitchen waste 46,774.88 (100%)		Excreta waste 146,800 (21.33%)	Straw waste 102,616.50 (34.38%)	

[a]: the contribution of wind, solar and biomass power is 57.37%, 17.12% and 25.51% respectively.
[b]: Power via HRES feed-in or direct feed-in is 58.68% and 41.32% respectively.

The hybrid wind-solar-biomass renewable energy system could feed in power to the main grid around 526 million kWh over the year among which wind power contributes above 57 %, and a quarter of the electricity is supplied by biomass power stations. The HRES project achieves annual net profits reaching above 135 million CNY. Biomass power stations, as followers, obtained around 140.71 million CNY per year and generated 228 million kWh of power, 58.68% of generated power feed into the main grid via the hybrid system. Over a long period, the current deployment could achieve good reliability, only a total of 2.92% of the agreed power has not been met to feed in the main grid over the whole year. From a social-environment perspective, carbon saving and job creation are value-adds in renewable energy development. 80.313 million and 16.301 million kg CO_2 emissions from fossil fuel generators could be avoided because of wind-solar and biomass power generation. The two stations provide 326.3 and 407 job opportunities per year. In addition, the biomass power station treats 46,774, 146,800 and 102,616 tons of kitchen, excreta, and straw wastes respectively over the year, with resourcing rates reaching 100%, 21.33% and 34.38%.

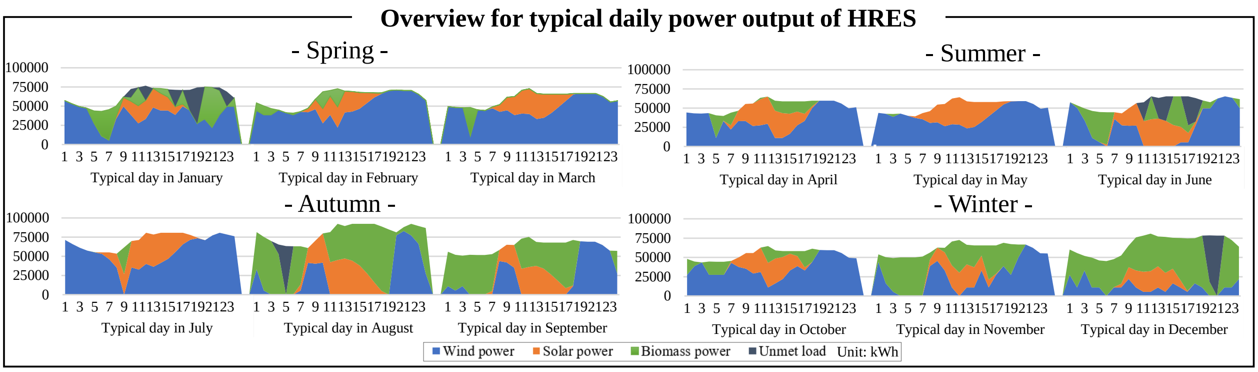

Figure 4: Real monthly wind-solar-biomass power output

Some differences would be observed between months during the study period. Fig. 4 presents a profile of the hourly power output on typical days over the year. Throughout the year, January, June, August, and December showed part of the agreed load not be fed, especially in June, when a total of 11.1% of the protocol output was not met, occurring from 10:00-11:00, 12:00-14:00 and 16:00-18:00. Further, biomass power trade is active in August, September, November, and December, because the straw waste would be generated after July, which is a high potential substrate for power generation.

4.4. *Validation of Result*

Some available real operation data of associated power stations in the Qianjiang area are used to compare with the optimal results in the basic case (Table 2) for the validation of applicability and efficiency for the developed methodology. First, the proposed model and solution program are recognized as objectives because the given deployment strategy set is the same as the actual operation of each power station. Further, economic benefits could be slightly improved under the same operation conditions for each wind-solar and biomass power supplier, proving the methodology's effectiveness in HRES deployment and operation optimization.

Table 2: Technological deployment and economic factors by optimization results and real operation data

Item	Facilities deployment				Levelized profit of Energy (CNY/kWh)	
	Wind turbines	photovoltaic panels	Anaerobic digestion	Gasification	Wind-solar	Biomass
Optimization result	3.6MW(14)&3.3MW(9)	1MW(100)	200 tons (1) &400 tons (1)	600 tons (1)	0.26	0.62
Real operation data	3.6MW(14)&3.3MW(9)	1MW(100)	200 tons (1) &400 tons (1)	600 tons (1)	0.24	0.56

4.5. *Influence of changing natural resources*

The influence of uncertain natural resources on stakeholders is analyzed by changing wind speed, solar irradiation, and biomass feedstock. Compared with the results of the tech-social performance, the profits and emission reduction see significant changes in this sensitive analysis, with the results shown in Fig. 5.

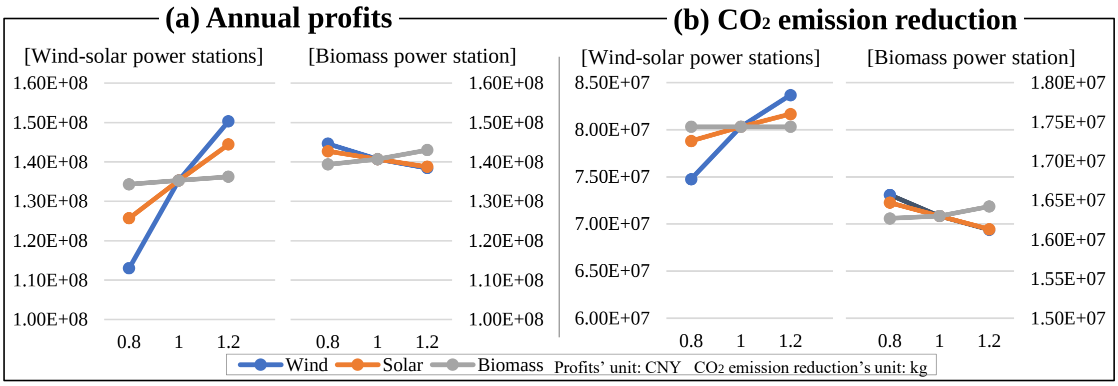

Figure 5: Annual profits and carbon emission reduction for stakeholders

Changes in wind speed are recognized as the main influence contributor towards each stakeholder both in the economy and environment. When the speed is varied from 80% of benchmark data to 120 % of it, the profit of the supplier of wind-solar power increases from 112.9 million to 135.3 million, reaching 150.3 million CNY finally. A similar positive correlation could be observed in solar radiation intensity. But for the operator of biomass power stations, the rising of the natural resource, including wind and solar, would drop their profits in the operation process, reducing by 6.17 million and 2.96 million CNY, respectively. The increase of waste as biomass feedstock could enhance the profits of the biomass power station while posing a slight influence on wind-solar power stations.

Fig. 5(b) shows the emission reduction performance changes as changing natural resources, showing a similar trend as profits. Noticeably, when the wind speed increases from 80% to the baseline value, the carbon abatement effect of wind-solar power station increases significantly by 5,562,288 kg, while the rate of the carbon reduction slows down after the wind speed continues to increase to 1.2 times the baseline value by only 3,365,389 kg. When the waste collection is increased from 80% to the baseline value for the biomass plant, the emission reduction efficiency is not significant, only from 16,270,215 to 16,301,859 kg. Still, if the waste collection potential is increased to 1.2 times the baseline, the emission reduction increases to 16,422,289 kg.

4.6. Influence of different agreed renewable power output strategies

To analyze the technological impact of the agreed output strategies, this subsection simulates both high and low agreed power output quantities as well as dynamic and constant feed-in patterns. Here, the monthly excess power and unserved load are compared under two given total power outputs with dynamic and constant feed-in strategies, where the dynamic strategy requires agreed power deliver varied as hourly demand load, setting as 16% and 18% of demand load (Fig. 6(a) and (b) respectively); and two constant strategies requires suppliers to feed-in fixed amount to the main grid per hour, maintained at 61,636 kWh and 69,340 kWh respectively (Fig 6(c) and (d)).

In the lower agreed power output amount scenario (Fig. 6(a) and (c)), dynamics strategies could present lower unserved load peak with monthly sums below 5 million KWh, but the more frequent compared with the constant strategy, shown in January, June, August, and December. In addition to December, natural resources, mainly wind power, would be wasted in each month shown as blue lines. Here the highest excess power is raised in May, peaking above 17 million kWh in the dynamics strategy and 20 million kWh in the constant feed-in strategy.

Compared with Fig. 6(a) and (c), the operator determined a larger agreed power output with the main grid, the unreliability of HRES (in Fig. 6(b)) increases when the total agreed power output is raised to 607,418,621 kWh to meet 18% of the hourly demand load. Especially in Jan, Jun, Aug, and Dec, the HRES is easily influenced, and the unserved load value fluctuates from 8.2 million to 10 million kWh. And if the constant strategy is considered (Fig. 6(d)), the reliability would be improved in January, August, and December, while the peak amount of unreliability becomes more in June, and a total of 10.5 million kWh.

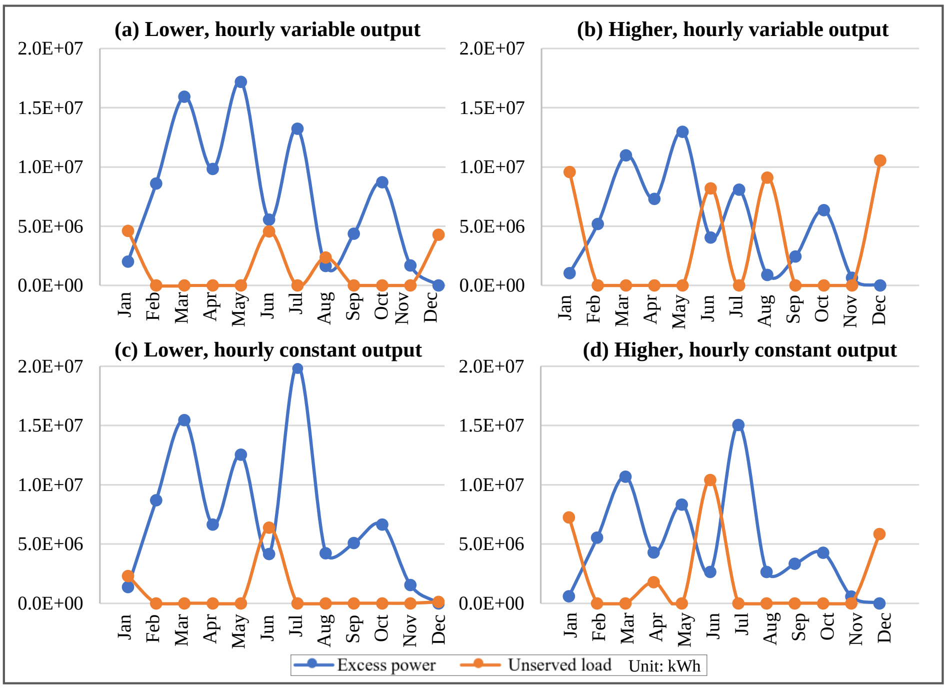

Figure 6: Monthly unserved load and excess power

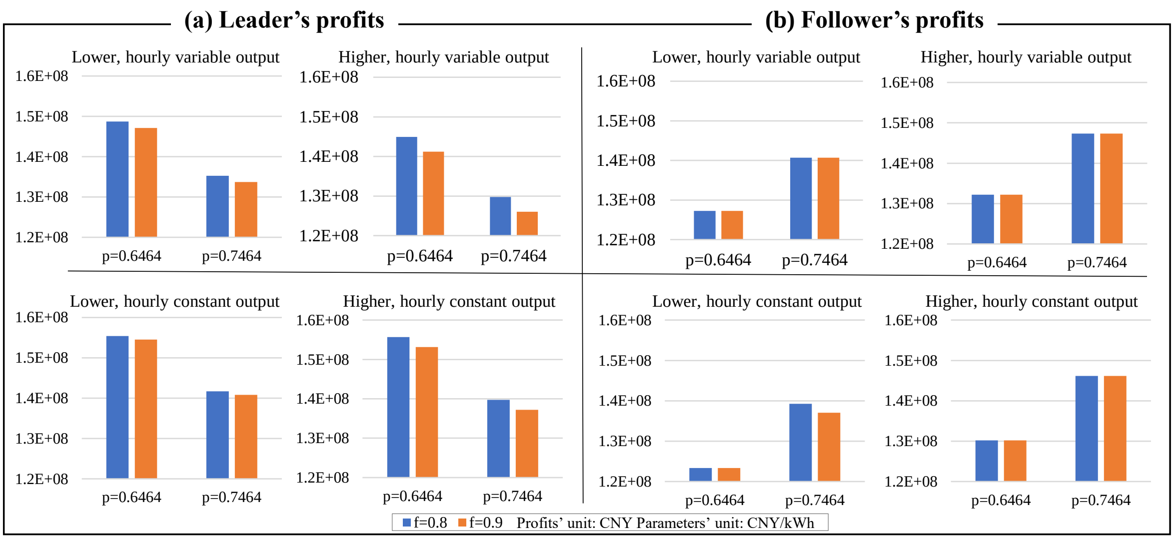

Figure 7: Total annual net profit of decision makers at upper and lower level

4.7. *Influence of different electricity price strategies*

In this subsection, the economic benefits of stakeholders are analyzed by adjusting the price of biomass power and the fine of unserved load power under different power feed-in strategies. There is a significant difference between decision-makers at upper and lower levels in power output strategies, in which the operator of HRES at the upper level achieves more profits if they choose the constant strategy. In contrast, profits for the biomass power station will be damaged.

In Fig. 7(a), the scenario of the constant feed-in mode with a lower output amount achieves the highest profit, at

155 million CNY, when the fine is set as 0.8 CNY/kWh and biomass power price is determined as 0.6464 CNY/kWh. But, if the dynamics high feed-in mode scenario is selected, the profits would drop to the lowest. In that scenario, if the unserved load fine is set at 0.8 CNY/kWh, 0.6464 CNY/kWh of purchase biomass price would be considered from the leader's view for profit-maximizing.

Fig. 7(b) sees the annual profit obtainable from the supplier of biomass power, where the profits would be improved if the HRES chooses the higher power output. And the lowest profit is shown in the scenario that the upper-level decision-maker determined the constant feed-in mode with a low power amount when the fine is 0.8 CNY/kWh with the 0.6464 CNY/kWh of biomass power price. And when HRES's operator chooses the variable power feed-in mode, it would pose a slight improvement compared with the constant strategy.

4.8. Related propositions

Based on the above analyses, the following conclusions were drawn.

(1) Integrating biomass power with solar-wind power is a win-win strategy for each stakeholder. From a global perspective, the integration strategy would significantly increase the operation benefits and reliability of the HRES, which allows suppliers of natural resource power to consider a larger amount of agreed power output. Larger profits, better environmental performance, and social benefits could be achieved because 25.51% of power as back-up of HRES could be provided from the biomass power station. Meanwhile, the profit per kWh of biomass power station could be improved by 0.06 CNY.

(2) Wind speed vary poses the largest influence on profits of the operator of the wind-solar power station. In this case, when wind speed increase from 0.8 to 1.0 of baseline, the profits could be improved by 19.75 %, and then if speed continues to increase, the marginal profit is diminishing, but it can still contribute a profit growth of 11.11%. In contrast, the increased availability of wind power has led to a reduction of 2.71% and 1.61% in the profitability of the biomass power station, mainly due to the reduced demand for biomass electricity in the proposed HRES.

(3) Power output strategies affect the reliability and resource utilization rate of HRES. The excess power presented in each period is different under the dynamic and constant output strategies. If the system chooses the variable feed-in according to demand load, the highest excess power is contributed in May, while in another strategy, the highest is in July. In addition, higher total agreed power output leads to a lower reliability performance and better resource utilization.

(4) Pricing of biomass power would directly influence decision-makers' profits at upper and lower levels. Compared with the fines on unserved power, the change in biomass power trade price would have a larger influence on profits requirement. In addition, the level of fines hardly not affects the profitability of biomass power stations.

(5) Constant feed-in strategy is better for HRES, while the dynamic feed-in mode is better for the biomass power stations. From Fig. 7, the highest profits of HRES are contributed by the constant feed-in mode with a lower power amount, presenting above 155 million CNY when p = 0.6464 CNY/kWh, f = 0.8~0.9 CNY/kWh. On the contrary, the highest profits of the biomass power stations are when the HRES chooses dynamics output mode as varied load demand, reaching 140 million and 147 million CNY when the power price is determined at 0.7464 CNY/kWh for lower and higher agreed power output respectively.

4.9. Application suggestions

Through discussion and analyses, some comprehensive suggestions are as follow:

(1) As a predictable and controllable backup, bioenergy should be integrated into the wind-solar hybrid renewable system. As proposition (1) mentioned, biomass power joined solar-wind hybrid renewable system could improve systematical profits and reliability, presenting more power output to satisfy energy demand and social-environmental benefits. Therefore, feasible measures such as attractive prices or policies should be explored to ensure that the collaboration strategy can be implemented in practice. It is worth noting that rice straw, as a highly seasonal waste, is characterized by storability; therefore, coordinating collection, storage, and resource recovery efforts throughout the year or even across years is necessary to increase bioenergy output.

(2) Reasonable pricing of biomass power should be determined in renewable electricity trading. In the game shown in the study, collaboration can be reached as long as the wind-solar power station offers a price comparable to that of the national grid. The biomass power station is willing to export stable power to help the wind-solar power station to achieve stable power output. As the price increases, the electricity output and the total profit will also increase.

Conversely, suppose the price is lower than the national grid's subsidy price for biomass power (0.6464 CNY/kWh). In that case, the collaboration will collapse, and the hybrid system and the main grid will suffer both technical and economic negative effects. Therefore, a reasonable price that combines the interests of many stakeholders is fundamental to attracting biomass energy into the HRES.

(3) January and June should be paid more attention to system robustness. Over the discussion in the basic case and sensitive analysis, it can be observed that regardless of the mode, the system failed to achieve the established output at certain times in January and June. In addition, the system operator needs to make targeted adjustments regarding the power output agreements during these two months to provide the main grid with the opportunity to react to ensure the security of the main grid. In addition, some months can be problematic due to the impact of different agreements. For example, under the variable output strategy, the system will also be less reliable in August and December. And if the total output is decided at a higher level and a constant output mode is adopted, the system stability will be affected at some moments in April.

(4) Operators of HRES should feed in the constant power output to the main grid per hour. That strategy could achieve more profits compared with a dynamic output agreement that varies with fluctuations in load demand, even though the total amount is the same. Moreover, if this model is chosen to supply the market demand, the total annual output power can be increased based same expected profits.

4.10. Comparison of results with previous work

Absolute justified comparison between studies is difficult because exact matching of configuration, load, and design parameters is not always possible. Therefore, comparing the optimal HRES results of the basic case with previous work is performed based on a similar configuration. Before the comparison, some common indicators were selected, and certain results were processed for some studies. Table 3 sees considerable reliability of the HRESs proposed, in which ULR could control below 4%. For economic items, because of different power generation amounts, research boundaries, and different subsidies implemented in each country, the levelized cost of energy without power selling revenue is used to compare economic benefits among these studies. This study presents the best economic benefit in power generation compared with existing literature with the highest power generation level. Correspondingly, the HRES proposed in this study saves the highest carbon emission because of the clean advantage of renewable energy. In comparison to studies of HRES fueled by 100% renewable energies, the present study's levelized cost of energy and reduction potential on carbon emission is better than Aziz et al. [70] and [71]. And reliability provided by the present study is higher than Li et al. [71].

Table 3: Comparison of the present study result with previous work

Ref.	Country	Hybrid renewable system		Total power generation	Renewable fraction	Unmet load rate	Levelized cost of energy	CO_2 reduction
		Basic component	Back-up	kWh/yr	(RF%)	(ULR%)	\$/kWh	kg/yr
Saiprasad et al. [72]	Australia	wind-solar	Li-Ion battery	5,006,840	75.68%	N/A	0.085	97,467.00
Bekele and Tadesse [73]	India	wind-solar-hydro	diesel generator	255,650	95.00%	1.50%	0.108	42,720.48
Aziz et al. [70]	Iraq	solar-hydro	battery	234,267	100.00%	0.44%	0.070	49,547.47
Li et al. [71]	China	solar-biomass	battery	699,545	100.00%	3.57%	0.240	1,297,174.00
Ahmad et al. [74]	Pakistan	wind-solar-biomass	fossil electricity	67,727,923	88.00%	N/A	0.053	19,976.61
Sawle et al. [75]	India	wind-solar-biomass	diesel-battery	73,109	96.82%	1.76%	0.195	N/A
Jia et al. [76]	China	wind-solar	biogas compressor	500,300	82.24%	N/A	0.067	138,541.00
Present Study	China	wind-solar	Biomass	526,071,983	100.00%	2.92%	0.040	80,313,980.92

5. Conclusion

Global economic development, growing total energy demand, and environmental concern triggered renewable electricity development. Electricity robustness needs to be focused on increasing renewable electricity because of the inevitable Intermittent of natural resources. Biomass resource as backup integrated HRES has been recognized as an efficient option for this problem, while the driver-contributed biomass to join HRES for integration has generally been ignored. Therefore, this study developed a Stackelberg-based biomass power trading framework for suppliers of multi-renewable powers to ensure that reliable power can eventually be delivered to the grid. In the framework, the operator of the wind-solar power station is a leader in purchasing biomass power at certain prices and determining their power generation for stable agreed power output and profit maximization; the biomass power station, as a follower, determines its operation strategies from waste collection to inventory and conversion, and trade distribution to achieve more operational profits. To simulate these operational strategies, a bi-level multi-objective dynamics optimization model was proposed to examine the specific relationships and activities of all stakeholders regarding technical feasibility, economic benefits, environmental sustainability, and social value in this hybrid 100% renewable energy system. Finally, the biomass power trading framework and optimization method were successfully simulated in solar-wind-biomass HRES in the Qianjiang area, Chongqing City. The results demonstrated the effectiveness of the proposed methodology. Levelized profits of energy reach 0.26 and 0.62 CNY/kWh for wind-solar power and biomass power, increased by 0.02 CNY and 0.06 CNY compared with real operation data. The sensitive analysis found that wind speed is the main influence factor in the operation of an HRES because it accounts for 57% of total power generation. In addition, different feed-in modes chosen by HRES's operator achieve different annual profits even though the total generation amount is the same, where the largest difference is expected to reach 11 million CNY.

To sum up, the main contribution of this work could be summarized as follow: (1) The biomass power trade game-based collaboration strategy guarantees the multi-renewable power integration for the reliability of HRES and utilization of natural resources; (2) the developed bi-level multi-objective optimization model not only allows decision makers to conduct optimal deployment respectively but also considers the effect of biomass power distribution on their own interests; (3) an efficient solving algorithm is capable of finding a mutually beneficial outcome for each stakeholder from the perspective of technological, economic, environmental and social perspectives; (4) successful application of methodology in the practice area provides a systematic optimization paradigm for optimization deployment of HRES fueled by 100% renewable energy, where exploration of the influence of biomass power joining, natural resource uncertainty, electricity price change, feed-in mode chosen on HRES deployment and operation, presents valuable proposition and suggestions as reference for the potential user in other geographical locations.

With the advantage of being flexible, this model allows users to determine the time period and starting point according to the practice case. In this study, the case spans a year-long starting in January, perfectly suited to the operational characteristics of HRES, especially those of wind and water resources. However, biomass resources, especially straw waste, are highly seasonal, and he will produce a large amount at a certain time period, so the subsequent ones may carry out a comparative case study with different starting times to analyze the impact of the generation time of biomass energy, on the operation of HRES throughout the year. In addition, this model sets the transaction volume as the decision variable and selects two different transaction prices for calculation and comparison in the sensitivity analysis. Afterward, transaction price and volume can be considered decision variables, so the constructed game is freer and more flexible. This involves nonlinear programming, which requires more complex solution procedures for subsequent analysis.

Acknowledgements

This research was supported by the National Social Science Fund of China [grant number 22&ZD142], and China Scholarship Council [grant number 202206240114].

Appendix A. Notations

Indices:

i	:	Wind power station index, where $i = 1, 2, \cdots, I$
j	:	Solar power station index, where $j = 1, 2, \cdots, J$
r	:	Biomass power station index, where $r = 1, 2, \cdots, R$
m	:	Waste type index, where $m = 1, 2, \cdots, M$
k	:	Month index, where $k = 1, 2, \cdots, K$
t	:	Time period index, where $t = 1, 2, \cdots, T$

Certain parameters:

A_i^w, A_j^s, A_r^b	:	Initial investment cost of unit wind turbine in station i, photovoltaic array in station j and biomass generator in station r
B_i^w, B_j^s, B_r^b	:	Replacement cost of a unit of wind turbine in station i, photovoltaic array in station j and biomass generator in station r
C_i^w, C_j^s, C_r^b	:	Operation and maintained cost of unit wind turbine in station i, photovoltaic array in station j and biomass generator in station r
$CRF_{(i,T)}, CRF_{(j,T)}$	:	Discount rate for station i and j
L_k	:	Number of days in month k
MR^m	:	unit management revenue for waste m
$n_i^{\max}, n_j^{\max}, n_r^{\max}, n_r^{Ho-max}$	:	Maximum number of wind turbines, PV arrays, biomass generators and warehouses that can be operated
$N_i^{\min}, N_i^{\max}$	:	Lower bounds and upper bounds in power output of wind power station i
$N_j^{\min}, N_j^{\max}$	:	Lower bounds and upper bounds in power output of solar power station i
p^w, p^s, p^b	:	Unit subsidy for wind, solar and bio power respectively
q_{sta}^w	:	Rated wind power output of a unit of wind turbines within rated wind speed range
q_{sta}^s	:	Rated solar power output of a unit of photovoltaic array under standard test condition
$\underline{q}_r^m, \overline{q}_r^m$	:	Lower bounds and upper bounds of waste disposal capacity in station r
$v_i(t)$	:	Actual wind speed at the height of hub at site i in month k at time period t
$v_i^{in}, v_i^{ra}, v_i^{out}$	:	Cut-in, rated and cut-out wind speed of the turbine
S_{kjt}, T_{kjt}	:	Actual solar radiation and ambient temperature at site j in month k at time period t
S_{sta}, T_{sta}	:	Solar radiation and ambient temperature under standard test condition
S_{kr}^m	:	Initial storage amount for waste m in station r in month k
T_i^w, T_j^s, T_r^b	:	Lifespan horizon for wind power station i, solar power station j and biomass generator in station r
$\overline{TE}^m(\widehat{d_{\cdot r}})$	:	Average transportation emission per ton waste m by station r
VC_r^m, VE_r^m	:	Unit cost/carbon emission of holding per ton waste m for one month in station r
DE_r^m	:	Unit carbon emission when unit waste m is treated in station r
JC_i, JC_j	:	Numbers of jobs created if the unit wind turbine with a rated capacity in station i and unit photovoltaic arra
JC_r^{Fa}, JC_r^{Ho}	:	Labor demand of waste facilities and warehouse facilities in station r with certain capacity
$\overline{TJ}^m(\widehat{d_{\cdot r}})$	:	The number of drivers needed to transport unit waste m in the area responsible for station r
$VS^m\%$	:	Total organic matter content (volatile solids) in waste m
$\varpi, \omega_i, \omega_j$	:	Unit carbon emission per kWh power from fossil fuel, wind turbines, and photovoltaic array respectively
τ	:	Temperature coefficient used in solar power generation
δ_r^m	:	Biofuel conversion factor from waste m of biomass power station r
ψ_r	:	Biomass power production factor of power station r
β	:	Power supplier's attitude parameter towards generation reliability
$\underline{S}_r^m, \overline{S}_r^m$	:	Total lower bounds and upper bounds in storage capacity in station r
ε^{URL}	:	Highest unmet load bound determined by operator of HRES
$\varepsilon^{CRu}, \varepsilon^{CRl}$	:	Lowest carbon emission reduction determined by operator of HRES/biomass power station
$\varepsilon^{JCu}, \varepsilon^{JCl}$	:	Lowest jobs creation determined by operator of HRES/biomass power station

Uncertain parameters:

$\widetilde{TD}_{kt}^E$	:	Residual loads at period time t in month k
$\widetilde{TD}_k^m$	:	Daily amount of generated waste m in month k.
$\overline{TC}^m(\widehat{d_{\cdot r}})$	:	Average unit transportation cost

Decision variables:

p^{b*} : Purchase price of biomass power determined between operators of HRES and biomass power station

$n^{w}_{ki}, n^{s}_{kj}, n^{b}_{kr}$: Actual number of wind turbines, photovoltaic arrays, biomass generators that are operated in month k at time period t

$Q^{HRES}_{kit}, Q^{HRES}_{kjt}, Q^{HRES}_{krt}$: Real power output of HRES which is provided by power stations i, j and r during time period t in a typical day of month k

Q^{BP}_{krt} : Power amount that is directly delivery to main grid by biomass power station r during time period t in a typical day of month k

$Q^{m(in)}_{kr}$: Daily incoming amount of waste m for station r in month k

Q^{m}_{krt} : Treatment amount of waste m in biomass power station r at period t in month k

OD^{E}_{kt} : Agreed load on time t in month k

UL_{kt} : Unserved load value of HRES at time t in month k

Appendix B. Associated data in the case

Table B.1: Technological-environmental details of various components.

Wind turbine	Rotor diameter 174 m	Hub height 100 m	Cut-in/out speed [5, 8] m/s	Rated speed 6.5 m/s	Carbon emission 0.02 kg/kWh
	Waste type	Organic matter content	Gas production	Calorific value of biofuels	Carbon emission*
Biogas generator	Kitchen waste	0.285	400 m^3/ton	5.2 kwh/m^3	49.69 kg/ton
	Excreta	0.164	500 m^3/ton	5.2 kWh/m^3	47.79 kg/ton
Snygas generator	Straw	0.54	1600 m^3/ton	1.38 kwh/m^3	65.11 kg/ton
Photovoltaic array	STC radiation 1 kW/m^3	STC temperature 25 ^oC	τ -0.35%/ ^oC	Carbon emission 0.037 kg/kWh	Main grid carbon emission 0.215 kg/kWh

Note: * - Carbon content of solid organic matter: 49.74%, 34.67%, and 41.92% respectively [77]
Source from Niu [78], Wang et al. [29], Zhejiang Windey Wind Power Co. [79], Baruah et al. [51], Luo et al. [80], Jia et al. [76]

Table B.2: Economic-social details of various components.

Component	Unit rated power	Available amount	Annual capital and replacement costs (CNY/yr)	Unit operation and maintenance costs (CNY/pm)	Job creation /facility	Life period (yrs)
Wind turbine	3.6 MW	14	5,787,936.00	84.50	9.72	25
	3.3 MW	9	3,410,748.00	84.50	8.91	25
Photovoltaic arrays	1 MW	100	15,853,214.00	84.50	1.10	20
Biogas generator	200 Tons/day	1	4,264,800.00	6.00	73.00	10
	400 Tons/day	1	6,397,200.00	6.00	109.50	10
Syngas generator	600 Tons/day	1	10,590,666.67	6.00	79.80	30

Source from Zhang [81], Baruah et al. [51], Wang et al. [29], Xu et al. [13]

Table B.3: Details related to waste collection and inventory

Waste collection	Management revenue (CNY/ton)	Transportation cost (CNY/ton)	Carbon emission (Kg/ton)	Job creation (jobs/(ton*yr))
Kitchen waste	110.00	(91.98, 101.92, 125.21)	22.95	1.05E-06
Excreta	134.00	(101.34, 122.43, 134.21)	36.98	1.69E-06
Straw	134.00	(109.2,122.12,132.34)	99.45	4.54E-06
Straw inventory	Inventory cost (CNY/(ton*day))	Carbon emission (Kg/ton)	Job creation (jobs/yr)	Capacity (Tons)
Warehouse park	750	(37.82, 38.23, 39.91)	(47.23, 48.32, 49.56)	36000[b]

[a]: Influenced by fuel price and Labour costs fluctuation, the data is collected in the triangular fuzzy number form and will be processed by the expectation method.
[b]: The warehouse cluster consists of three three-story buildings with a total area of 3772 m^2.

Reference

[1] G. Liu, Z. Qin, T. Diao, X. Wang, P. Wang, X. Bai, Low carbon economic dispatch of biogas-wind-solar renewable energy system based on robust stochastic optimization 139 (2022) 108069, ISSN 01420615, doi:10.1016/j.ijepes.2022.108069, URL https://linkinghub.elsevier.com/retrieve/pii/S0142061522001119.

[2] S. Ghaem Sigarchian, R. Paleta, A. Malmquist, A. Pina, Feasibility study of using a biogas engine as backup in a decentralized hybrid (PV/wind/battery) power generation system - Case study Kenya 90 (2015-10) 1830–1841, ISSN 03605442, doi:10.1016/j.energy.2015.07.008, URL https://linkinghub.elsevier.com/retrieve/pii/S0360544215009020.

[3] M. I. Hoffert, K. Caldeira, G. Benford, D. R. Criswell, C. Green, H. Herzog, A. K. Jain, H. S. Kheshgi, K. S. Lackner, J. S. Lewis, H. D. Lightfoot, W. Manheimer, J. C. Mankins, M. E. Mauel, L. J. Perkins, M. E. Schlesinger, T. Volk, T. M. L. Wigley, Advanced Technology Paths to Global Climate Stability: Energy for a Greenhouse Planet 298 (5595) (2002) 981–987, ISSN 0036-8075, 1095-9203, doi:10.1126/science.1072357, URL https://www.science.org/doi/10.1126/science.1072357.

[4] S. Afrane, J. D. Ampah, C. Jin, H. Liu, E. M. Aboagye, Techno-economic feasibility of waste-to-energy technologies for investment in Ghana: A multicriteria assessment based on fuzzy TOPSIS approach, Journal of Cleaner Production 318 (2021) 128515.

[5] S. E. Hosseini, Transition away from fossil fuels toward renewables: lessons from Russia-Ukraine crisis, Future Energy 01 (2022) 02–05.

[6] X. Xu, H. Jia, H.-D. Chiang, D. C. Yu, D. Wang, Dynamic Modeling and Interaction of Hybrid Natural Gas and Electricity Supply System in Microgrid, IEEE Transactions on Power Systems 30 (3) (2015) 1212–1221, doi:10.1109/TPWRS.2014.2343021.

[7] T. Sarkar, A. Bhattacharjee, H. Samanta, K. Bhattacharya, H. Saha, Optimal design and implementation of solar PV-wind-biogas-VRFB storage integrated smart hybrid microgrid for ensuring zero loss of power supply probability 191 (2019) 102–118, ISSN 01968904, doi:10.1016/j.enconman.2019.04.025, URL https://linkinghub.elsevier.com/retrieve/pii/S0196890419304376.

[8] F. J. Ardakani, M. M. Ardehali, Long-term electrical energy consumption forecasting for developing and developed economies based on different optimized models and historical data types 65 (2014) 452–461, ISSN 0360-5442, doi:https://doi.org/10.1016/j.energy.2013.12.031, URL https://www.sciencedirect.com/science/article/pii/S0360544213010888.

[9] K. Mould, F. Silva, S. F. Knott, B. O'Regan, A comparative analysis of biogas and hydrogen, and the impact of the certificates and blockchain new paradigms 47 (93) (2022) 39303–39318, ISSN 03603199, doi:10.1016/j.ijhydene.2022.09.107, URL https://linkinghub.elsevier.com/retrieve/pii/S036031992204246X.

[10] A. Colmenar-Santos, J.-L. Bonilla-Gmez, D. Borge-Diez, M. Castro-Gil, Hybridization of concentrated solar power plants with biogas production systems as an alternative to premiums: The case of Spain 47 (2015) 186–197, ISSN 13640321, doi:10.1016/j.rser.2015.03.061, URL https://linkinghub.elsevier.com/retrieve/pii/S1364032115002142.

[11] S. Sinha, S. Chandel, Review of software tools for hybrid renewable energy systems, Renewable and Sustainable Energy Reviews 32 (2014) 192–205, ISSN 1364-0321, doi:https://doi.org/10.1016/j.rser.2014.01.035, URL https://www.sciencedirect.com/science/article/pii/S136403211400046X.

[12] P. K. Kushwaha, P. Ray, C. Bhattacharjee, Optimal sizing of a hybrid renewable energy system: A socio-techno-economic-environmental perspective, Journal of Solar Energy Engineering 145 (3) (2023) 031003.

[13] J. Xu, Y. Huang, Y. Shi, R. Li, Reverse supply chain management approach for municipal solid waste with waste sorting subsidy policy, Socio-Economic Planning Sciences 81 (2022) 101180, ISSN 0038-0121, doi:https://doi.org/10.1016/j.seps.2021.101180, URL https://www.sciencedirect.com/science/article/pii/S0038012121001725.

[14] N. Zhao, F. You, Dairy waste-to-energy incentive policy design using Stackelberg-game-based modeling and optimization, Applied Energy 254 (2019) 113701, ISSN 0306-2619, doi:https://doi.org/10.1016/j.apenergy.2019.113701, URL https://www.sciencedirect.com/science/article/pii/S0306261919313881.

[15] L. Ma, N. Liu, H. Sun, C. Li, W. Liu, Bi-level frequency regulation resource trading for Electricity Consumers: A Data-driven contract approach, International Journal of Electrical Power & Energy Systems 135 (2022) 107543, ISSN 0142-0615, doi:https://doi.org/10.1016/j.ijepes.2021.107543, URL https://www.sciencedirect.com/science/article/pii/S0142061521007808.

[16] S. E. Ahmadi, D. Sadeghi, M. Marzband, A. Abusorrah, K. Sedraoui, Decentralized bi-level stochastic optimization approach for multi-agent multi-energy networked micro-grids with multi-energy storage tech-

nologies, Energy 245 (2022) 123223, ISSN 0360-5442, doi:https://doi.org/10.1016/j.energy.2022.123223, URL https://www.sciencedirect.com/science/article/pii/S0360544222001268.

[17] R. Sharifi, A. Anvari-Moghaddam, S. H. Fathi, V. Vahidinasab, A bi-level model for strategic bidding of a price-maker retailer with flexible demands in day-ahead electricity market, International Journal of Electrical Power & Energy Systems 121 (2020) 106065, ISSN 0142-0615, doi:https://doi.org/10.1016/j.ijepes.2020.106065, URL https://www.sciencedirect.com/science/article/pii/S0142061519335276.

[18] D. Yue, F. You, Stackelberg-game-based modeling and optimization for supply chain design and operations: A mixed integer bilevel programming framework, Computers & Chemical Engineering 102 (2017) 81–95, ISSN 0098-1354, doi:https://doi.org/10.1016/j.compchemeng.2016.07.026, URL https://www.sciencedirect.com/science/article/pii/S0098135416302460, sustainability & Energy Systems.

[19] I. Soares, M. J. Alves, C. H. Antunes, Designing time-of-use tariffs in electricity retail markets using a bi-level model C Estimating bounds when the lower level problem cannot be exactly solved, Omega 93 (2020) 102027, ISSN 0305-0483, doi:https://doi.org/10.1016/j.omega.2019.01.005, URL https://www.sciencedirect.com/science/article/pii/S0305048318306819.

[20] Z. Hua, J. Li, B. Zhou, S. W. Or, K. W. Chan, Y. Meng, Game-theoretic multi-energy trading framework for strategic biogas-solar renewable energy provider with heterogeneous consumers 260 (2022) 125018, ISSN 03605442, doi:10.1016/j.energy.2022.125018, URL https://linkinghub.elsevier.com/retrieve/pii/S0360544222019156.

[21] A. Couto, A. Estanqueiro, Enhancing wind power forecast accuracy using the weather research and forecasting numerical model-based features and artificial neuronal networks, Renewable Energy 201 (2022) 1076–1085, ISSN 0960-1481, doi:https://doi.org/10.1016/j.renene.2022.11.022, URL https://www.sciencedirect.com/science/article/pii/S096014812201655X.

[22] C. L. Dewangan, S. Singh, S. Chakrabarti, Combining forecasts of day-ahead solar power, Energy 202 (2020) 117743, ISSN 0360-5442, doi:https://doi.org/10.1016/j.energy.2020.117743, URL https://www.sciencedirect.com/science/article/pii/S0360544220308501.

[23] A. Cano, P. Arvalo, F. Jurado, Energy analysis and techno-economic assessment of a hybrid PV/HKT/BAT system using biomass gasifier: Cuenca-Ecuador case study, Energy 202 (2020) 117727, ISSN 0360-5442, doi:https://doi.org/10.1016/j.energy.2020.117727, URL https://www.sciencedirect.com/science/article/pii/S0360544220308343.

[24] L. B. van Leeuwen, H. J. Cappon, K. J. Keesman, Urban bio-waste as a flexible source of electricity in a fully renewable energy system, Biomass and Bioenergy 145 (2021) 105931, ISSN 0961-9534, doi:https://doi.org/10.1016/j.biombioe.2020.105931, URL https://www.sciencedirect.com/science/article/pii/S0961953420304578.

[25] Y. Wei, Z. Li, W. Ran, H. Yuan, X. Li, Performance and microbial community dynamics in anaerobic co-digestion of chicken manure and corn stover with different modification methods and trace element supplementation strategy, Bioresource Technology 325 (2021) 124713, ISSN 0960-8524, doi:https://doi.org/10.1016/j.biortech.2021.124713, URL https://www.sciencedirect.com/science/article/pii/S0960852421000511.

[26] X. Zhu, D. Yellezuome, R. Liu, Z. Wang, X. Liu, Effects of co-digestion of food waste, corn straw and chicken manure in two-stage anaerobic digestion on trace element bioavailability and microbial community composition, Bioresource Technology 346 (2022) 126625, ISSN 0960-8524, doi:https://doi.org/10.1016/j.biortech.2021.126625, URL https://www.sciencedirect.com/science/article/pii/S0960852421019672.

[27] Y. Q. Ang, A. Polly, A. Kulkarni, G. B. Chambi, M. Hernandez, M. N. Haji, Multi-objective optimization of hybrid renewable energy systems with urban building energy modeling for a prototypical coastal community 201 (2022) 72–84, ISSN 09601481, doi: 10.1016/j.renene.2022.09.126, URL https://linkinghub.elsevier.com/retrieve/pii/S0960148122014859.

[28] R. Chaurasia, S. Gairola, Y. Pal, Technical, economic, and environmental performance comparison analysis of a hybrid renewable energy system based on power dispatch strategies, Sustainable Energy Technologies and Assessments 53 (2022) 102787, ISSN 2213-1388, doi: https://doi.org/10.1016/j.seta.2022.102787, URL https://www.sciencedirect.com/science/article/pii/S2213138822008359.

[29] F. Wang, J. Xu, L. Liu, G. Yin, J. Wang, J. Yan, Optimal design and operation of hybrid renewable energy system for drinking water treatment, Energy 219 (2021) 119673, ISSN 0360-5442, doi:https://doi.org/10.1016/j.energy.2020.119673, URL https://www.sciencedirect.com/science/article/pii/S0360544220327808.

[30] F. Wang, Y. Xie, J. Xu, Reliable-economical equilibrium based short-term scheduling towards hybrid hydro-photovoltaic generation systems: Case study from China, Applied Energy 253 (2019) 113559, ISSN 0306-2619, doi:https://doi.org/10.1016/j.apenergy.2019.113559, URL https://www.sciencedirect.com/science/article/pii/S0306261919312334.

[31] Y. He, S. Guo, J. Zhou, G. Song, A. Kurban, H. Wang, The multi-stage framework for optimal sizing and operation of hybrid electrical-thermal energy storage system, Energy 245 (2022) 123248, ISSN 0360-5442, doi:https://doi.org/10.1016/j.energy.2022.123248, URL https://www.sciencedirect.com/science/article/pii/S0360544222001517.

[32] W. Zhang, A. Maleki, M. A. Rosen, J. Liu, Sizing a stand-alone solar-wind-hydrogen energy system using weather forecasting and a hybrid search optimization algorithm, Energy Conversion and Management 180 (2019) 609–621, ISSN 0196-8904, doi:https://doi.org/10.1016/j.enconman.2018.08.102, URL https://www.sciencedirect.com/science/article/pii/S0196890418309671.

[33] P. Liu, L. Liu, X. Xu, Y. Zhao, J. Niu, Q. Zhang, Carbon footprint and carbon emission intensity of grassland wind farms in Inner Mongolia, Journal of Cleaner Production 313 (2021) 127878, ISSN 0959-6526, doi:https://doi.org/10.1016/j.jclepro.2021.127878, URL https://www.sciencedirect.com/science/article/pii/S0959652621020965.

[34] E. Santoyo-Castelazo, A. Azapagic, Sustainability assessment of energy systems: integrating environmental, economic and social aspects, Journal of Cleaner Production 80 (2014) 119–138, ISSN 0959-6526, doi:https://doi.org/10.1016/j.jclepro.2014.05.061, URL https://www.sciencedirect.com/science/article/pii/S0959652614005381.

[35] P. K. Kushwaha, C. Bhattacharjee, Integrated techno-economic-enviro-socio design of the hybrid renewable energy system with suitable dispatch strategy for domestic and telecommunication load across India, Journal of Energy Storage 55 (2022) 105340.

[36] M. Thirunavukkarasu, Y. Sawle, H. Lala, A comprehensive review on optimization of hybrid renewable energy systems using various optimization techniques, Renewable and Sustainable Energy Reviews 176 (2023) 113192.
[37] R. Dufo-López, I. R. Cristóbal-Monreal, J. M. Yusta, Optimisation of PV-wind-diesel-battery stand-alone systems to minimise cost and maximise human development index and job creation, Renewable Energy 94 (2016) 280–293.
[38] A. Mostafaeipour, Feasibility study of harnessing wind energy for turbine installation in province of Yazd in Iran, Renewable and Sustainable Energy Reviews 14 (1) (2010) 93–111, ISSN 1364-0321, doi:https://doi.org/10.1016/j.rser.2009.05.009, URL `https://www.sciencedirect.com/science/article/pii/S1364032109001117`.
[39] R. Hassan, B. K. Das, M. Hasan, Integrated off-grid hybrid renewable energy system optimization based on economic, environmental, and social indicators for sustainable development, Energy 250 (2022) 123823, ISSN 0360-5442, doi:https://doi.org/10.1016/j.energy.2022.123823, URL `https://www.sciencedirect.com/science/article/pii/S0360544222007265`.
[40] M. R. Akhtari, M. Baneshi, Techno-economic assessment and optimization of a hybrid renewable co-supply of electricity, heat and hydrogen system to enhance performance by recovering excess electricity for a large energy consumer, Energy Conversion and Management 188 (2019) 131–141, ISSN 0196-8904, doi:https://doi.org/10.1016/j.enconman.2019.03.067, URL `https://www.sciencedirect.com/science/article/pii/S0196890419303723`.
[41] F. Li, J. Qiu, Multi-objective optimization for integrated hydroCphotovoltaic power system, Applied Energy 167 (2016) 377–384, ISSN 0306-2619, doi:https://doi.org/10.1016/j.apenergy.2015.09.018, URL `https://www.sciencedirect.com/science/article/pii/S0306261915010880`.
[42] S. Wang, S. Wang, J. Wu, B. Zhang, L. Lv, A multi-objective nonlinear planning model of biomass power generation for supporting subsidy policies optimization, Energy Reports 7 (2021) 7060–7071, ISSN 2352-4847, doi:https://doi.org/10.1016/j.egyr.2021.09.069, URL `https://www.sciencedirect.com/science/article/pii/S2352484721008751`.
[43] World Coal Association (WCA), COAL FACTS, 2022.
[44] National bureau of statistics of China (NBSC), China Statistical Yearbook in 2022, 2022.
[45] H. Nandimandalam, A. Aghalari, V. G. Gude, M. Marufuzzaman, Multi-objective optimization model for regional renewable biomass supported electricity generation in rural regions, Energy Conversion and Management 266 (2022) 115833, ISSN 0196-8904, doi:https://doi.org/10.1016/j.enconman.2022.115833, URL `https://www.sciencedirect.com/science/article/pii/S019689042200629X`.
[46] F. Zhang, D. M. Johnson, J. Wang, Integrating multimodal transport into forest-delivered biofuel supply chain design, Renewable Energy 93 (2016) 58–67, ISSN 0960-1481, doi:https://doi.org/10.1016/j.renene.2016.02.047, URL `https://www.sciencedirect.com/science/article/pii/S0960148116301483`.
[47] M. S. Roni, S. D. Eksioglu, K. G. Cafferty, J. J. Jacobson, A multi-objective, hub-and-spoke model to design and manage biofuel supply chains, Annals of Operations Research 249 (1-2) (2017) 351–380.
[48] D. Yue, M. Slivinsky, J. Sumpter, F. You, Sustainable design and operation of cellulosic bioelectricity supply chain networks with life cycle economic, environmental, and social optimization, Industrial & Engineering Chemistry Research 53 (10) (2014) 4008–4029.
[49] Y. Huang, J. Xu, Bi-level multi-objective programming approach for bioenergy production optimization towards co-digestion of kitchen waste and rice straw, Fuel 316 (2022) 123117, ISSN 0016-2361, doi:https://doi.org/10.1016/j.fuel.2021.123117, URL `https://www.sciencedirect.com/science/article/pii/S0016236121029768`.
[50] A. M. Argo, E. C. Tan, D. Inman, M. H. Langholtz, L. M. Eaton, J. J. Jacobson, C. T. Wright, D. J. Muth Jr, M. M. Wu, Y.-W. Chiu, et al., Investigation of biochemical biorefinery sizing and environmental sustainability impacts for conventional bale system and advanced uniform biomass logistics designs, Biofuels, Bioproducts and Biorefining 7 (3) (2013) 282–302.
[51] A. Baruah, M. Basu, D. Amuley, Modeling of an autonomous hybrid renewable energy system for electrification of a township: A case study for Sikkim, India, Renewable and Sustainable Energy Reviews 135 (2021) 110158, ISSN 1364-0321, doi: https://doi.org/10.1016/j.rser.2020.110158, URL `https://www.sciencedirect.com/science/article/pii/S1364032120304494`.
[52] Y. Huang, Y. Shi, J. Xu, Integrated district electricity system with anaerobic digestion and gasification for bioenergy production optimization and carbon reduction, Sustainable Energy Technologies and Assessments 55 (2023) 102890, ISSN 2213-1388, doi: https://doi.org/10.1016/j.seta.2022.102890, URL `https://www.sciencedirect.com/science/article/pii/S2213138822009389`.
[53] F. Habibi, E. Asadi, S. J. Sadjadi, F. Barzinpour, A multi-objective robust optimization model for site-selection and capacity allocation of municipal solid waste facilities: A case study in Tehran, Journal of cleaner production 166 (2017) 816–834.
[54] M. Rabbani, K. R. Mokarrari, N. Akbarian-saravi, A multi-objective location inventory routing problem with pricing decisions in a sustainable waste management system, Sustainable Cities and Society 75 (2021) 103319, ISSN 2210-6707, doi: https://doi.org/10.1016/j.scs.2021.103319, URL `https://www.sciencedirect.com/science/article/pii/S2210670721005953`.
[55] S. Pouriani, E. Asadi-Gangraj, M. M. Paydar, A robust bi-level optimization modelling approach for municipal solid waste management: a real case study of Iran, Journal of cleaner production 240 (10) (2019) 118125.
[56] J. Nash, Non-cooperative games, Ann Math 54 (2) (1951) 286–95.
[57] V. Chankong, Y. Y. Haimes, Multiobjective decision making: theory and methodology, Courier Dover Publications, 2008.
[58] O. Ben-Ayed, C. E. Blair, Computational Difficulties of Bilevel Linear Programming, Operations Research 38 (3) (1990) 556–560, doi: 10.1287/opre.38.3.556, URL `https://doi.org/10.1287/opre.38.3.556`.
[59] J. Xu, L. Fan, Y. Xie, G. Wu, Recycling-equilibrium strategy for phosphogypsum pollution control in phosphate fertilizer plants, Journal of Cleaner Production 215 (APR.1) (2019) 175–197.
[60] B. Colson, P. Marcotte, G. Savard, An overview of bilevel optimization, Annals of Operations Research 153 (2007) 235–256.
[61] M. A. Hanson, On sufficiency of the Kuhn-Tucker conditions, Journal of Mathematical Analysis and Applications 80 (2) (1981) 545 – 550, ISSN 0022-247X, doi:https://doi.org/10.1016/0022-247X(81)90123-2, URL `http://www.sciencedirect.com/science/article/pii/0022247X81901232`.
[62] Q. Huang, J. Xu, Bi-level multi-objective programming approach for carbon emission quota allocation towards co-combustion of coal and sewage sludge, Energy 211.
[63] Qianjiang District People's Government, Qianjiang District Health Development "14-5" Plan, 2021.

[64] World Bank Group, PV Electricity and solar radiation, URL https://globalsolaratlas.info/detail?c=29.699664,107.858277,9&s=29.274421,108 2022.

[65] China National Development and Reform Commission, Notice of National Development and Reform Commission on Improving the Feed-in Tariff Policy for Wind Power, URL https://zfxxgk.ndrc.gov.cn/web/iteminfo.jsp?id=16185, 2019.

[66] China National Development and Reform Commission, National Development and Reform Commission on the improvement of photovoltaic power generation grid tariff mechanism Notice of relevant issues, URL https://www.ndrc.gov.cn/xxgk/zcfb/tz/201904/t20190430_962433.html?code=&state=123, 2019.

[67] Chongqing Development and Reform Commission, Chongqing Municipal Development and Reform Commission on matters related to deepening the market reform of the city's coal-fired power generation feed-in tariff, URL http://fzggw.cq.gov.cn/zwgk/zfxxgkml/zcjd/202111/t20211108_9937479.html, 2021.

[68] Y. Zhu, S. Lin, Y. Ye, M. Ke, Overview of Feed-in Tariffs and Subsidy Policies for Biomass Power Generation, URL https://baijiahao.baidu.com/s?id=1689942928121816659&wfr=spider&for=pc, 2021.

[69] J. Xu, F. Wang, et al., Economic-environmental equilibrium based optimal scheduling strategy towards wind-solar-thermal power generation system under limited resources, Applied Energy 231 (2018) 355–371.

[70] A. S. Aziz, M. F. N. Tajuddin, M. R. Adzman, A. Azmi, M. A. Ramli, Optimization and sensitivity analysis of standalone hybrid energy systems for rural electrification: A case study of Iraq, Renewable Energy 138 (2019) 775–792, ISSN 0960-1481, doi:https://doi.org/10.1016/j.renene.2019.02.004, URL https://www.sciencedirect.com/science/article/pii/S096014811930148X.

[71] C. Li, L. Zhang, F. Qiu, R. Fu, Optimization and enviro-economic assessment of hybrid sustainable energy systems: The case study of a photovoltaic/biogas/diesel/battery system in Xuzhou, China, Energy Strategy Reviews 41 (2022) 100852, ISSN 2211-467X, doi: https://doi.org/10.1016/j.esr.2022.100852, URL https://www.sciencedirect.com/science/article/pii/S2211467X22000505.

[72] N. Saiprasad, A. Kalam, A. Zayegh, Optimal sizing of renewable energy system for a university in Australia, in: 2017 Australasian Universities Power Engineering Conference (AUPEC), 1–6, doi:10.1109/AUPEC.2017.8282483, 2017.

[73] G. Bekele, G. Tadesse, Feasibility study of small Hydro/PV/Wind hybrid system for off-grid rural electrification in Ethiopia, Applied Energy 97 (2012) 5–15, ISSN 0306-2619, doi:https://doi.org/10.1016/j.apenergy.2011.11.059, URL https://www.sciencedirect.com/science/article/pii/S0306261911007653, energy Solutions for a Sustainable World - Proceedings of the Third International Conference on Applied Energy, May 16-18, 2011 - Perugia, Italy.

[74] J. Ahmad, M. Imran, A. Khalid, W. Iqbal, S. R. Ashraf, M. Adnan, S. F. Ali, K. S. Khokhar, Techno economic analysis of a wind-photovoltaic-biomass hybrid renewable energy system for rural electrification: A case study of Kallar Kahar, Energy 148 (2018) 208–234, ISSN 0360-5442, doi:https://doi.org/10.1016/j.energy.2018.01.133, URL https://www.sciencedirect.com/science/article/pii/S0360544218301610.

[75] Y. Sawle, S. Gupta, A. K. Bohre, Socio-techno-economic design of hybrid renewable energy system using optimization techniques, Renewable Energy 119 (2018) 459–472, ISSN 0960-1481, doi:https://doi.org/10.1016/j.renene.2017.11.058, URL https://www.sciencedirect.com/science/article/pii/S096014811731159X.

[76] K. Jia, C. Liu, S. Li, D. Jiang, Modeling and optimization of a hybrid renewable energy system integrated with gas turbine and energy storage, Energy Conversion and Management 279 (2023) 116763, ISSN 0196-8904, doi:https://doi.org/10.1016/j.enconman.2023.116763, URL https://www.sciencedirect.com/science/article/pii/S0196890423001097.

[77] W. Zhang, T. Kong, W. Xing, R. Li, T. Yang, N. Yao, D. Lv, Links between carbon/nitrogen ratio, synergy and microbial characteristics of long-term semi-continuous anaerobic co-digestion of food waste, cattle manure and corn straw, Bioresource Technology 343 (2022) 126094, ISSN 0960-8524, doi:https://doi.org/10.1016/j.biortech.2021.126094, URL https://www.sciencedirect.com/science/article/pii/S096085242101436X.

[78] T. Niu, The first set of wind turbine tower manufacturing proje ct of Chongqing Qianjiang Wufuling wind farm project (80MW) was successfully lifted, URL https://wind.in-en.com/html/wind-2409440.shtml, 2021.

[79] Zhejiang Windey Wind Power Co., Product center of windey group, URL https://www.chinawindey.com/product.aspx, 2020.

[80] X. Luo, Y. Liu, X. Liu, Bi-level multi-objective optimization of design and subsidies for standalone hybrid renewable energy systems: a novel approach based on artificial neural network, Journal of Building Engineering 41 (2021) 102744.

[81] N. Zhang, 3037~3300 RMB/kW, Goldwind, Yunda and Mingyang win bids for 3 wind turbine projects in CGN, URL http://www.nengyuancn.com/news/05901.html, 2021.